energies

MDPI

Review

Lithium-Ion Capacitors: A Review of Design and Active Materials

Jacob J. Lamb and Odne S. Burheim *

Department of Energy and Process Engineering and ENERSENSE, Faculty of Engineering, Norwegian University of Science and Technology (NTNU), 7491 Trondheim, Norway; jacob.j.lamb@ntnu.no
* Correspondence: odne.s.burheim@ntnu.no

Abstract: Lithium-ion capacitors (LICs) have gained significant attention in recent years for their increased energy density without altering their power density. LICs achieve higher capacitance than traditional supercapacitors due to their hybrid battery electrode and subsequent higher voltage. This is due to the asymmetric action of LICs, which serves as an enhancer of traditional supercapacitors. This culminates in the potential for pollution-free, long-lasting, and efficient energy-storing that is required to realise a renewable energy future. This review article offers an analysis of recent progress in the production of LIC electrode active materials, requirements and performance. In-situ hybridisation and ex-situ recombination of composite materials comprising a wide variety of active constituents is also addressed. The possible challenges and opportunities for future research based on LICs in energy applications are also discussed.

Keywords: lithium-ion capacitors; nodes; cathodes; oxides; carbon; silicon

Citation: Lamb, J.J.; Burheim, O.S. Lithium-Ion Capacitors: A Review of Design and Active Materials. *Energies* **2021**, *14*, 979. https://doi.org/10.3390/en14040979

Academic Editor: Woojin Choi

Received: 5 January 2021
Accepted: 11 February 2021
Published: 12 February 2021

1. Introduction

Due to the rapid growth of renewable energy production recently [1], there is a significant requirement for electrical energy storage technologies. Energy storage offers the ability to moderate the variability of electrical energy [2]. This represents a rapidly emerging market for energy storage that is currently underutilised. The characteristics of the energy storage needs, in general, are electro-compatibility and will relate more specifically to cheap and highly efficient storage solutions for stationary purposes, and energy and power intensity for the transport and transmission sector (to which lithium-based batteries are the answer). In addition, there is a need for shifting the current battery production from fossil-based energy to renewables to reduce the embedded emissions of energy storage systems. Moreover, the materials required in the production of energy storage system should ideally originate from areas free of geopolitical conflicts, child labour, corruption and environment unfriendly excavation and extraction methods [3]. In this light, lithium-ion batteries (LIBs) utilising ethically mined materials and energy produced by renewables have huge international market advantages when considering environmental, social and corporate governance (ESG) aspects.

Lithium-ion capacitors (LICs) were first produced in 2001 by Amatucci et al. [4]. LICs are considered one of the most effective devices for storing energy and are often seen as an offspring from LIBs for several reasons. In addition, Sodium-ion and Potassium-ion capacitors (SIC and KIC, respectively), have also become of commercial interest as they similarly are a hybrid device combining an ion battery with a traditional capacitor. This review will focus on the LIC developments as the main example of a hybrid capacitor, but it must be noted that there are many similarities between LICs, NICs and KICs. LIBs normally have high energy density (>150 W h kg^{-1}) and have no memory impact as in conventional Ni-Cd/Ni-MH batteries [5,6]. Despite this, their low power density (<1 kW kg^{-1}), and lower cycle life and capacity loss [7] hinders their utilisation in some applications. By comparison, LICs can provide high power density (>10 kW kg^{-1}) and long cycle life (usually >5000 cycles); however, their comparatively low energy density

(5–10 W h kg^{-1}) restricts their applications in certain fields (LIC applications have been thoroughly discussed in [8–10]). To close the performance gap between LIBs and traditional capacitors, LICs have been developed to incorporate the strengths of both LIBs and traditional capacitors [6,11–14].

By practice, LIBs consist of a metal oxide cathode, separator, electrolyte, and a Lithium-based anode. In contrast, non-aqueous liquid electrolyte LICs with high power densities (>10 kW kg^{-1}) and long-term cyclic durability (10,000–100,000 cycles), are ideal for large-scale energy storage [5,15]. Typical LIC designs use a high-capacity battery-type electrode and a high-rate capacitor-type electrode [5,16]. During the charge-discharge cycle, charges are deposited concurrently and asymmetrically in the LIC by surface ion adsorption/desorption on the capacitor-type electrode and Li^+ intercalation/de-intercalation on the battery-type electrode, respectively [17,18]. It is worth noting that the battery- and capacitor-type electrodes of the LIC system work in various potential windows, which may expand the range of operating voltage of LICs and contribute to high energy density.

Supercapacitors can be classified into asymmetric supercapacitors, pseudo-capacitors (PCs) and electric double-layer capacitors (EDLCs) depending on the charging storage mechanisms [19]. PCs store energy using the fast redox reaction on the surface of the electrode components, such as metal oxides, metal sulphides and polymer conductors. Whereas energy storage on the surface of the porous carbon with a large specific surface area (SSA) is accomplished through strong ion absorption and desorption for EDLCs.

LIBs operate through Li^+ that travels back and forth between the electrodes followed by the electrode materials' bulk redox reaction. The combination of the positive EDLC electrode and the negative LIB electrode forms a LIC, reducing the deficiencies in both LICs and LIBs. LICs may typically be categorised as dual-carbon, non-carbon, and mixed forms, distinguished by whether or not the electrodes contain carbon materials. The densities of energy and power of LICs depend primarily on the configuration of electrode materials in the devices [17,20]. The most promising industrial prospects are for dual-carbon LICs (DC-LICs), in which both electrodes are composed of carbon materials. Owing to the surplus and low carbon levels, the average expense of DC-LICs may be effectively popular.

Until now, owing to their strong gravimetric functional potential and excellent electrochemical operation, a number of components, such as metal compounds, polyanions and metalloid/metal compounds, have been produced in LICs for battery-type electrodes [21]. However, their further production in LICs is constrained by the poor conductivity, wide volume variability and strong polarisation of these active materials [5]. Carbonaceous materials have been extensively researched and used in energy storage fields like LICs [22–25], benefiting from low expense, sufficient supplies, plenty of allotropes and transformations as well as superior physical/chemical stability. Because of their large specific surface region, strong conductivity and excellent usability to electrolytes, carbon materials were also inserted into the electrodes to solve such issues [26,27]. Furthermore, carbon compounds may also specifically function as the active compounds of battery-type electrodes in LICs, since they have active Li^+ intercalation/de-intercalation sites [28,29].

Unlike battery-type electrodes, LICs counter-electrodes are capacitor-type. Consequently, numerous porous carbon materials with a wide specific surface region, such as activated carbon (AC) and graphene are potential candidates for LICs capacitor-type electrodes [30,31]. Their capacitances rely primarily on the surface of carbon-based electrodes [32] for the adsorption/desorption of ions. Therefore, porous structures with sufficient distribution of pore size play an important role in the electrochemical production of carbon materials in LICs [33,34]. Specific materials are typically inserted into the carbonaceous materials to have pseudo-capacity to further improve the capacitance of the capacitor-type electrode.

In this review, we will identify the fundamental active materials used for LICs and analyse electrode/capacitor-type carbon-based battery-based electrode materials over many decades. By concentrating on the most common cases with industrial potential, we demonstrate the main components of LICs. The knowledge gaps and future trends

associated with LICs are also addressed, which provides a detailed insight into the potential areas of further research of LIC active materials.

2. Lithium-Ion Capacitor Fundamentals

Throughout the consumer electronics, automobile, aerospace and stationary industries, electrical energy-storage devices play a key function. There are several types of reversible electrochemical energy storage systems in the format of accumulators, flow cell systems, secondary batteries (rechargeable) and primary batteries (single-use). In terms of secondary and primary batteries, the former has a lower energy intensity while the latter offers better power; however, the cyclable nature of secondary batteries makes them ideal for use as an energy storage solution. The current prevailing technology is LIBs. Large LIBs have a gravimetric energy upwards of 200 Wh kg^{-1}, and with an overall effective power density of up to 350 W kg^{-1}. In comparison, most industrial electrochemical capacitors have average power density as high as 10 kW kg^{-1}, and with gravimetric energy of up to 7 Wh kg^{-1} [2]. Figure 1 gives an overview of the power and energy densities of ultracapacitors and LIBs compared to other energy storage technologies. A common target for advanced electrical energy storage systems is to provide high energy as well as high power in a single system [35–38]. A LIC is a comparatively modern system, intermediate in energy between batteries and supercapacitors, though giving supercapacitor-like power and cyclability properties.

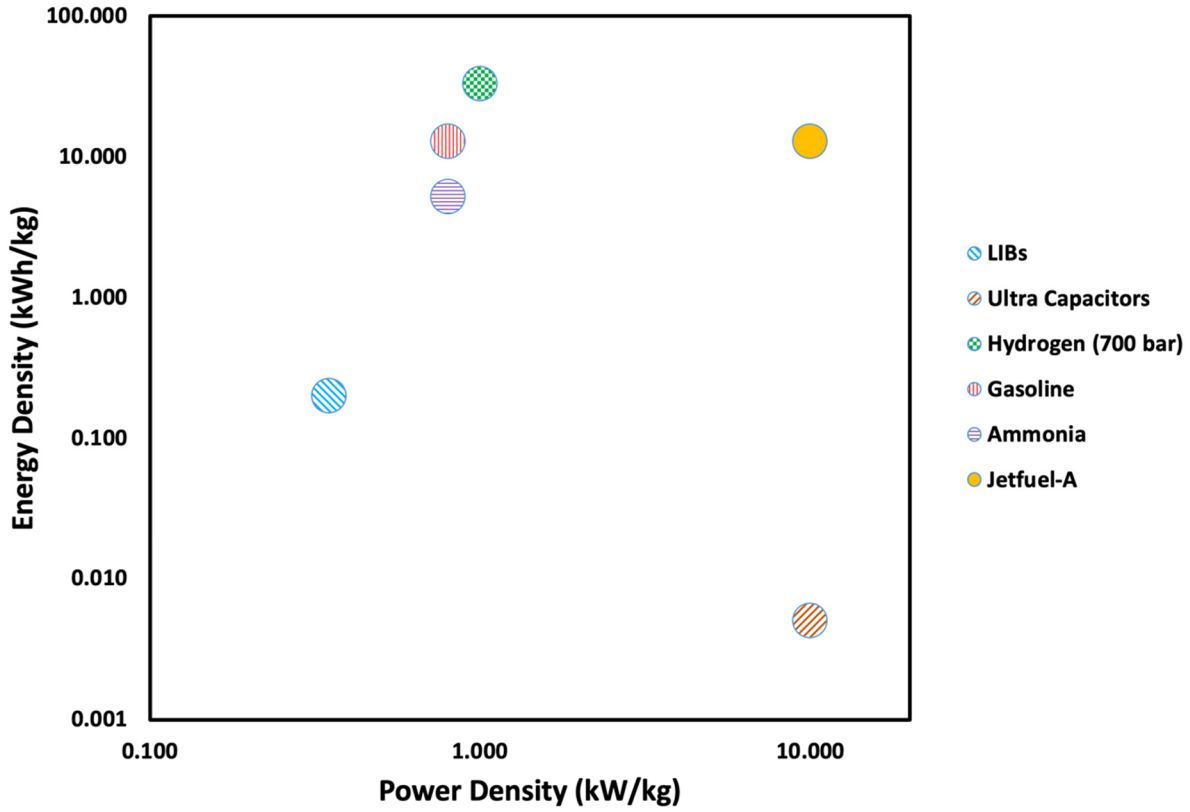

Figure 1. Ragone plot of current LIB, hydrogen, gasoline, ammonia and jet fuel—energy storage solutions in comparison to traditional industrial ultracapacitors.

It is important to define the components of LICs before recognising the basic energy storage function of the LICs. As a kind of asymmetric supercapacitor, LICs usually consist of a battery-type electrode with the insertion/extraction of lithium ions and a pseudo-capacitance or ion adsorption/desorption capacitor-type electrode [39,40]. As the battery-type electrode does not only serve as an anode but also as a cathode, LICs have been previously separated into two types [41]:

1. The battery-like electrode acts as the anode, and the capacitor-like electrode acts as the cathode. Anions are usually absorbed on the porous surface or defects that may be apparent on the cathode during the charge cycle, whereas Li^+ ions are intercalated (as Li) in the active anode.
2. The capacitor-type electrode functions as the anode and the battery-type electrode functions as the cathode. Li^+ de-intercalates from the cathode during the charging phase. Li^+ immediately migrates in the electrolyte and adsorbs on the anode. This requires some redox reaction at the cathode (e.g., cathode oxidation: $LiCoO_2 \rightarrow Li^+ + e^- + Li^-$-$CoO_2$; and, anode reduction: Li^++C_6-graphite + $e^- \rightarrow LiC_6$-graphite).

Regenerative braking and grid stabilisers are significant possible end-uses of the LICs. Regenerative braking energy recovery from cars, heavy-duty engines, and increasingly light-duty vehicles represents a major potential opportunity that is not completely explored due to the shortcomings of current secondary battery and supercapacitor technologies (electrochemical capacitor and ultracapacitor). On-board regenerative braking is a possible mechanism to restore a significant fraction of the energy [42]. LICs do not have the inherent density of energy-storage needed for economic and spatially effective implementation. In comparison, LIBs do not have enough capacity, which needs a charge rate of up to 200 C (1 C is 1 h charge, 200 C is 18 s charge), or around 100 times larger size than what is required for just breaking adsorption.

LICs form a new class of devices capable of bridging the output of commercial EDLC supercapacitors and traditional LIBs [5,15,20]. As previously discussed, LICs are capable of producing 4 to 5 times higher energy values than EDLC ultracapacitors. This superior capacity is obtained by depending on a carbonate-based battery electrolyte that generates a higher voltage of the unit than acetonitrile (4.2 V vs. 2.7 V). Although 5000 cycles is a substantial lifetime for a LIB, they cannot be implemented in place of an ultracapacitor. This is because ultracapacitors run continuously up to thousands of charges per day in some cases. Therefore, LICs appear ideal to replace ultracapacitor electrochemical technologies.

Typically, while the battery-type electrode acts as an anode (case 1 above), it needs to be pre-lithiated during production before being implemented in a LICs, which may bring the anode's capacity closer to that of Li [43,44]. Pre-lithiation is a method used for LIBs and LICs to compensate for the potential loss of active lithium so higher reversible potentials and higher gravimetric energies are obtained. It is achieved by storage of a certain amount of active lithium in the anode prior to the cells first charge/discharge cycle. There are many methods available for pre-lithiation and can be performed to the active material or the electrode as a whole [45]. As a consequence, a LICs working voltage can raise and even exceed 4.5 V. The energy density is compared by their capacitance and the operating voltage [39,46], as typically chosen comparable specific energy units are V, kJ/mol and kWh/kg. The energy efficiency of LICs can be significantly enhanced due to the large working voltage of the battery-type electrodes. That is, with constant operating currents and resistances (*rj*-loss), this efficiency reduction becomes relatively less significant by increasing the open-circuit voltage (efficiency = $(E_{ocp}$-$rj)/E_{ocp}$). Nevertheless, a phase transition frequently follows the faradaic reaction of the battery-type electrode, which results in a weak rate efficiency, lower cycle life and slow dynamics [46–49]. To overcome these issues, the incorporation of highly conductive carbonaceous additives such as graphene, carbon nanotubes (CNTs) and AC are important in addition to the production of nanoscale-structured electrodes to obtain improved electronic conductivity [50–52].

Unlike the pure battery-type electrode, reversible ion adsorption or rapid redox reactions occurs on the capacitor-type electrode sheet, which provides the possibility that LICs have comparable power density to that of ultracapacitors by integrating an effective battery-type electrode with strong kinetics [53]. Also essential to their functional implementation is the cycling efficiency of LICs. Besides the inherent behaviour of the electrode of the battery type and the electrode of the capacitor-type, the mass ratio between the electrode of the battery type and the electrode of the capacitor-type often plays a crucial role in the cycle life of the LIC.

The charges for an asymmetric cell should be distributed at both electrodes (i.e., $Q_{anode} = Q_{cath}$). The charges deposited are aligned with the electrode's basic potential (C) and mass (m) ($Q \propto C \times \Delta E \times m$) [54,55]. The optimal mass ratio between the battery-type electrode and the capacitor-type electrode can therefore be determined by the following equation [56]:

$$\frac{m_{cath}}{m_{anode}} = \frac{C_{anode} \times \Delta E_{anode}}{C_{cath} \times \Delta E_{cath}} \quad (1)$$

where the electrode mass, the basic capacitance and the voltage range in the load/discharge phase for the anode and the cathode are m, C and ΔE, respectively. Nonetheless, the capacitance of the capacitor-type electrode is significantly smaller compared to that of the battery-type electrode [23,31]. Therefore, the manufacturing of high-density carbon products (e.g., micro- and macro-carbon composites), is the primary aim in the production of advanced LICs.

Two techniques are typically used to improve the natural capacitance of capacitor-type electrodes: construction of capacitor-type electrodes with broad natural surface area and incorporation of pseudocapacitive or heteroatom doping materials [57,58]. As described above, carbon products, either as active products or as conductive additives, perform irreplaceable roles in the applications of LICs due to the excellent intra- or inter-particle conductivity and the outstanding electrolyte accessibility [59–62].

3. Electrode Materials

Nanostructured carbons are significant LIC materials used either independently or in conjunction with a second active step of Li such as TiO_2. Yao et al [59] published a review of the carbons used in LICs (Table 1). The carbons are often rich in heteroatoms (especially oxygen) and contain varying degrees of graphene ordering. For carbon allotropes, extremely deficient or heteroatomic carbons do not fall into the classic taxonomy, but instead reflect the similarity of structure and chemistry between pure graphite/graphene and completely amorphous activated carbon. Lithium deposition is typically poorly known in nongraphic carbons, except at fairly high concentrations typical of a battery. The charge levels expected by hybrid devices are far less known and require further research.

3.1. Anodes

3.1.1. Carbon Materials

Graphite, with a hexagonal mesh structure made from carbon atoms, has been used in consumer LIBs goods as a negative electrode material since 1991 [63]. Graphite will provide a large plateau power around 300 mAh g^{-1} below 0.2 V and will guarantee a secure charge-discharge plateau. Alternatively, graphite suffers from a low rate capability induced by the strong crystallinity and anisotropy that further limits the power density [6]. To increase the capacity of graphite, ball milling, extremely conductive carbon surface grinding, graphisation degree regulation, and the application of defects and additives are all used [64–66].

Graphitised carbon, for which the space and microstructures of the interlayer can be conveniently modified, has the most interesting perspectives for use in anodes of LICs. The coexistence of graphical structures and amorphous structures allows graphised carbon to successfully combine a high plateau potential and superior rate efficiency. Catalytic graphisation with the aid of a metal-ions is an important process for preparing graphised carbon under fairly mild conditions (<1200 °C) [67]. The degree of graphitisation can be regulated by adjusting the temperature, precursor and catalyst structures.

Table 1. Carbonaceous material-based lithium-ion capacitor (LIC) summary.

Configuration (Anode//Cathode)	Voltage	Max Energy (Wh/kg) at Power (W/kg)	Energy (Wh/kg) at Max Power (W/kg)	Cyclability
N-doped carbon nanopipes//reduced graphene oxides [68]	0–4 V	262 at 450	78 at 9000	91% over 4000 cycles
graphene//armored graphene [69]	0–4.3 V	160 at 900	59 at 19,000	89% over 1000 cycles
microcrystalline graphite//mesoporous carbon nanospheres/graphene [70]	2.2–4.2 V	80 at 152	32 at 11,600	93% over 4000 cycles
reduced GO//resin-derived carbon combined with GO [71]	0–4 V	148.3 at 150	45 at 6500	79% over 3000 cycles
B&N-doped carbon nanofiber//B&N-doped carbon nanofiber [32]	0–4.5 V	220 at 225	104 at 22,500	81% over 5000 cycles
graphite//activated graphene [72]	2–4 V	147.8	Not reported	Not reported
graphite//functionalised graphene [73]	2–4 V	106 at 84	85 at 4200	100% over 1000 cycles
hard carbon//activated carbon [74]	1.4–4.3 V	80 at 150	65 at 2350	82% over 10,000 cycles
hard carbon//bioderived mesoporous carbon [75,76]	1.7–4.2 V	121 at 300	50 at 9000	81% over 8000 cycles
graphite//activated carbon [72]	1.5–5 V	145.8 at 65	18 at 18,000	65% over 10,000 cycles
hard carbon//activated carbon [77]	2–4 V	82 at 100	14 at 20,000	97% over 600 cycles
graphite//graphene [78]	2–4 V	135 at 50	105 at 1500	97% over 3500 cycles
N-doped hard carbon//activated carbon [79]	2–4 V	28.5 at 348	13.1 at 6940	97% over 5000 cycles
soft carbon//activated carbon [76]	0–4.4 V	115 at 25	16 at 15,000	63% over 15,000 cycles
graphene//activated carbon [80]	2–4 V	95 at 27	61.7 at 222.2	74% over 300 cycles
graphite//activated carbon [81]	2–4 V	103	Not reported	77% over 100 cycles

Hard carbon is a suitable choice for high power LICs [64,77,82], with better kinetics and a greater space distance between the carbon layers than graphite. Zhang et al. [83] contrasted the impact of LIC output on two specific hard carbon materials (spherical and irregular hard carbon) with an AC cathode, observing that the irregular hard carbon exhibited optimum electrochemical efficiency with a high energy density of up to 85.7 W h kg^{-1} and a power density of up to 7.6 kW kg^{-1} centred on the active material mass of two electrodes in the voltage range of 2–4 V. Furthermore, preparation of a hard carbon anode extracted from a carbonaceous source, such as a nitrogen-doped carbonised polyimide microsphere (CPIMS) [79], can also be a feasible solution. Despite this, the voltage hysteresis and sloping characteristics during hard carbon charging/discharge are unfavourable to the cycling stability of LICs. Sun et al. [84] extensively examined the electrochemical efficiency and power fading behaviours of hard carbon LICs and noticed that power fading of LICs during cycling was induced by a rise in internal resistance and a depletion of lithium deposited on the anode.

Benefiting from the superior mobility of electron carriers and strong lithium-ion transport kinetics, graphene is also a promising candidate as an anode material, rather than being used exclusively as a cathode material [15]. Ren et al. [80] fabricated pre-lithiated graphene nanosheets in LICs as an anode, providing a cumulative power density of 220 W kg^{-1} at an energy density of 62 W h kg^{-1} with a capacity retention of 74 % at 400 mA g^{-1} after 300 cycles.

Ahn et al. [85] provided a highly oriented graphene sponge (HOG) with an ultra-high energy density as an anode. The AC/HOG LICs demonstrated 3.6 times greater diffusivity of the lithium-ion than the AC/graphitized carbon LICs. As a result, they obtained large energy densities of 232 at 57 W kg^{-1} and 131.9 W h kg^{-1} at 2.8 kW kg^{-1}. In a DC-LICs device with AC as the cathode, Phattharasupakun et al. [86] documented a nitrogen-doped reduced graphene oxide (N-rGO) aerogel anode. They exhibited a maximum specific energy of 170.28 W h kg^{-1} in the voltage range of 2.0–4.0 V, and the average power density exceeded 25.75 kW kg^{-1} after 2000 cycles with almost no decay in efficiency.

Composites processing is an efficient way to combine multiple forms of carbon materials (e.g., graphite, hard carbon and graphene.) as an active substrate for producing high-performance LIC materials. Lim et al. [66] recorded high energy intensity and high power intensity DC-LICs, using natural graphite-coated hard carbon as anode materials. The DC-LIC achieved improved densities in energy and strength, as well as enhanced cycling efficiency.

3.1.2. Transition Metal Materials

Standard transition metal oxides, including $Li_4Ti_5O_{12}$, TiO_2, Nb_2O_5, Fe_2O_3 and SnO_2, have been extensively studied as anodes of LICs due to their large abundance and strong basic gravimetric potential [87–91]. Despite this, most transition metal oxides typically experience a phase change during the charge/discharge cycle, which is seen by the plateaus in the galvanostatic charge–discharge curves and strong peaks in the CV profiles. These phase transitions can result in broad volume growth, resulting in a negative impact on the integrity of electrodes, resulting in low cycling efficiency. Nevertheless, the composition of TiO_2 and $Li_4Ti_5O_{12}$ during reversible lithium intercalation/extraction is more robust. The integration of such transition metal oxides into porous carbon materials would solve or mitigate the above issues to achieve hybrid architectures. A recent review by Liu et al. [92] gives a comprehensive overview of transition metal LICs. Table 2 gives an overview of transition metals used in LIC electrode design.

Table 2. Transition metal-based LIC summary.

Configuration (Anode//Cathode)	Voltage	Max Energy (Wh/kg) at Power (W/kg)	Energy (Wh/kg) at Max Power (W/kg)	Cyclability
TiO_2 hollow spheres at graphene//graphene [93]	0–3 V	72 at 303	10 at 2000	65% over 1000 cycles
TiO_2 at mesoporous carbon//AC [94]	0–3 V	67.4 at 75	27.5 at 5000	80.5% over 10,000 cycles
TiO_2 nanobelt arrays//graphene hydrogels [95]	0–3.8 V	82 at 570	21 at 19,000	73% over 600 cycles
TiO_2 at rGO//AC [87]	1–3 V	42 at 800	8.9 at 8000	Not reported
TiO_2–CNT//active carbon [96]	1–3 V	59.6 at 120	31.2 at 13,900	Not reported
$Li_4Ti_5O_{12}$–CNT//graphene foam [97]	1–3.6 V	101.8 at 436.1	12.7 at 12,300	84.8% over 5000 cycles
$Li_4Ti_5O_{12}$//reduced graphene oxide [98]	1–3 V	45 at 400	30 at 3300	100% over 5000 cycles
nanocrystalline $Li_4Ti_5O_{12}$//active carbon [99]	1.5–3 V	55 at 64.6	28.8 at 10,300	Not reported
TiO_2-coated $Li_4Ti_5O_{12}$//active carbon [100]	0.5–2.5 V	74.85 at 300	36 at 7500	83.3% over 5000 cycles
$Li_4Ti_5O_{12}$//N-doped porous carbon [101]	1–3 V	63 at 200	16 at 5000	Not reported
graphene-$Li_4Ti_5O_{12}$//graphene-sucrose [102]	0–3 V	95 at 45	32 at 3000	94% over 500 cycles
spheres $Li_4Ti_5O_{12}$//active carbon [103]	1–3.5 V	74.3 at 156.26	41.7 at 468.7	93% over 500 cycles
graphene-wrapped $Li_4Ti_5O_{12}$//active carbon [104]	1–2.5 V	50 at 16	15 at 2500	75% over 1000 cycles

3.1.3. Polyanion and Carbon Composites

Typically, the $Li_3V_2(PO_4)_3$, developed with VO_6 octahedra and PO_4 tetrahedra corner-sharing, crystallises in a monoclinical configuration. The comparatively broad gap space of these crystals allows for the quick diffusion and reaction kinetics of different lithium sites. Because $Li_3V_2(PO_4)_3$ content is an amphoteric powder that can be either decreased by lithium injection or oxidised by lithium elimination, the electrochemical efficiency of both low (1.0–3.0 V) and high (3.0–4.3 V) voltage applications for $Li_3V_2(PO_4)_3$ has been studied [105]. These were observed to provide maximum energy densities between 27 and 25 W h kg^{-1}, respectively. Unlike $Li_3V_2(PO_4)_3$, $LiTi_2(PO_4)_3$ has a NASICON-type frame structure, which consists of PO_4 tetrahedra bound by octahedral unit corners of TiO_6. Each of the PO_4 tetrahedrons are connected to four octahedral TiO_6 units, and in effect a TiO_6 unit is connected to six PO_4 tetrahedrons, allowing for multiple ionic replacements at various lattices [41]. Cyclic voltammetry calculation was observed with a two-phase reaction process at 2.38 V during Li-insertion and an extraction at 2.60 V. As a result,

the LICs based on $LiTi_2(PO_4)_3$ carbon-coated anodes display ultra-high energy and power densities of 14 W h kg^{-1} and 180 W kg^{-1}, respectively [106].

For LIC anodes, $TiNb_2O_7$ will serve as an alternate nominee for $Li_4Ti_5O_{12}$. $TiNb_2O_7$'s monoclinical crystal structure comprises of disordered Nb and Ti atoms, which may have two-dimensional interstitial spaces for rapid Li-ion injection and show an energy density of 110.4 W h kg^{-1} at 99.58 W kg^{-1} [107]. Importantly, the $TiNb_2O_7$ on C electrode's Li injection activity was analysed in detail and the pseudo-capacitive reaction mechanism for intercalation was achieved [41].

3.1.4. Metalloid/Carbon and Metal Materials

The production and materials used for sustainable LICs manufacturing is becoming increasingly important. The use of silicon within carbon electrodes provide a promising route for sustainable LIC production in the future. Silicon is particularly of interest due to it being the second most abundant element in the Earth's crust. Due to its low lithiation ability (<0.5 V) and strong real theoretical efficiency (4200 mAh g^{-1}), Si is a promising material for high-performance LIC anodes [108,109]. Despite its excellent load-discharge platforms and extremely high specific capacity, its cycling and rate performance may be poor due to its severe volume expansion and low electronic and ionic conductivity [110]. Furthermore, due to its inherent semi-conductive design, the low conductivity may also restrict its performance in charge/discharge at high current density [111–113].

Composite processing is an efficient way to combine multiple forms of active materials as an active substrate for producing high-performance LIC materials. Soft carbon is a frequently used commercial anode material with high conductivity, fast lithium-ion transport and long cycling performance, but its specific capacity and operating platform still require improvement. Therefore, using a small amount of silicon-carbon composite in a soft carbon anode could ameliorate the anode's charge/discharge kinetics and also provide surplus lithium to slow the rate of active lithium consumption in long-term cycling after anode pre-lithiation. Using this approach, it has been observed that such a LIC has over 95% capacitance retention after 10,000 cycles at 20 °C [110].

Based on 3-electrode hybrid configuration [77], other types of lithium, such as lithium silicide, can be used for the anodes [114]. Pre-lithiation has traditionally been done on the anode; however, pre-lithiation on the cathode has been observed, which in turn is contradictory to how LIBs are produced [115]. That would be potentially better because the system is instead constructed in a thermodynamically stable manner (which may not be the case with a symmetric unit, e.g., a carbon–carbon LIC).

Sn has a greater electrical conductivity relative to Si, which will contribute to Sn anodes showing a higher rate capacity. Nevertheless, during the charge/discharge phase, Sn also suffers from a significant volume shift which can result in extreme polarisation of the electrode material [116–118]. The construction of tiny Sn nanoparticles with a binding carbon substratum is currently a successful method for overcoming these problems.

3.2. Cathodes

In the early research into LICs, activated carbon was dominantly used as the cathode material with a focus on the energy-storage process of surface adsorption. This was because it shows a large surface area (33,000 m_2 g^{-1}), excellent conductivity (almost 60 S m^{-1}) and strong chemical stability [41]. An AC cathode's energy storage capability also provides a power of approximately 50 mAh g^{-1} [41]. Compared with anode electrode performance, it is comparatively smaller. For load-balance, the cathode's mass load is typically two to four times that of the anode, depending on the cathode and anode's different capacitances [41]. Amatucci et al. [4] produced a LIC system using AC as the cathode, and nanostructured $Li_4Ti_5O_{12}$ (LTO) as the anode, the first use of AC in LICs. The voltage window of LICs in an organic electrolyte dependent on AC cathodes has since been designed in the range of 1.5–4.5 V to ensure high energy density and preserve the long cycle stability of LICs [72].

Additionally, carbon derived from metal-organic frameworks (MOF) with various architectures has also been widely researched in LICs. For example, large surface area (2714 m_2 g^{-1}) carbon cuboids were synthesised by pyrolysing the zinc-based MOF-5, which exhibits a peculiar crumpled-sheet porous morphology assembled with the required micro and mesoporosity values [119]. The MOF-dependent LIC provides a maximum effective energy density of 65 W h kg^{-1} with excellent power capacity, dependent on the advanced structure. Likewise, polyhedral hollow carbon derived from MOF was also produced and used in LICs [120]. It is worth noting that the removal of metal ions during the preparation of MOF-derived carbon is a required step due to the presence of metal ions in the MOF precursor.

Graphene's unique 2D structure and physical properties and its derivatives make them distinctive building blocks for producing various porous 3D architectures. Thanks to the combination of porous structures and the excellent intrinsic properties of graphene and its derivatives, these 3D architectures exhibit excellent chemical stability and strong specific surface area as well as fast electron transport kinetics. Therefore, these high-performance 3D architectures are strong candidates for use as the cathodes of LICs. Various techniques for constructing graphene-based architectures for LICs have been comprehensively documented in recent years [13,41,63,98]. Importantly, integrating microporous carbon with surface connectivity into graphene structures is an important technique for further increasing the LIC's strength and energy densities.

4. Design of Lithium-Ion Capacitors

In terms of LIC design, the process of pre-lithiation, the working voltage and the mass ratio of the cathode to the anode allow a difference in energy capacity, power efficiency and cyclic stability. An ideal working capacity can usually be accomplished by intercalating Li^+ into the interlayer of graphite. In this way, it is possible to achieve reduced electrode resistance, increased energy density and stable cycling efficiency [63]. A very critical element in maintaining power equilibrium is the mass ratio of the cathode to the anode (m+/m−). Taking into account the aforementioned criteria, finding a compromise between the correct degree of pre-lithiation, an effective functioning voltage window and the optimum m+/m− is of considerable importance. Although some researchers perform pre-lithiation on one or both of the electrodes, others depend entirely on Li in the electrolyte (e.g., from $LiPF_6$), resulting in reduced performance due to the loss of active Li [59,121,122]. The need for a solid electrolyte interface (SEI), its creation, continuous growth and cracking is a major problem correlated with the usage of carbon anodes. During cycling, one will need to hold the SEI steady and prevent Li plating that involves careful regulation of the negative electrode voltage, temperature and effective current density. Therefore, a carbon–carbon design requires an asymmetric mass loading with the weight of the lower-capacity adsorption carbon cathode being up to 5 times higher than that for the lithium-containing anode.

4.1. Pre-Lithiation Strategy

During the production of LICs, a pre-lithiation cycle is performed to the active material or whole electrode of the anode guarantee that it operates at fairly low potential and to supply lithium ions for the anode-side insertion/extraction reaction. In turn, the added lithium through pre-lithiation reduces the electrode resistance and accounts for the permanent active lithium loss during cycles induced by the creation of solid electrolyte interface films (SEI) on the anode. The following can be performed using distinctive pre-lithiation approaches [13,30,45,63]: the electrochemical process (ECP); the short-circuit pre-lithiation through external short-circuit (ESC) and internal short-circuit (ISC) methods; the introduction of permanent lithium transition metal oxides (LTMOs) on the cathode side; and, the application of sacrificial lithium chloride to the electrolyte. Pre-lithiation methods can also be adapted between different capacitor chemistries (e.g., LIC, NIC and KIC) [123]. Jin et al. (2020) give a thorough review of pre-lithiation technologies in LICs, outlining the current progress and perspectives [124].

An important step in creating high-performance LIC systems is the pre-lithiation of the electrodes. According to the restricted solubility of salts such as $LiPF_6$ or $NaClO_4$ in carbonate solvents, permanent ion loss results in ionic conductivity degradation [63]. During prolonged cycling, devices focused on non-lithiated electrodes have been shown to have decreased lithium ion content in the electrolyte, significantly deteriorating the overall LIC potential [81,121]. Besides SEI, Li can be trapped in the majority of electrode materials (e.g., hard carbons) [125]. Pre-charging at least one electrode is a key element in evaluating a hybrid device's output in terms of initial energy, power conservation and cycling conservation [63]. A study of Ragone properties typically shows that, in addition to the electrolyte [80,81,126,127], systems at the peak of the energy–power range are those that utilise a secondary supply of ions.

This training compensates for the depletion of the Li ion induced by initial SEI forming and permanent bulk trapping. As long as there is no substantial increase in SEI and bulk trapping during cycling, the concentration of electrolytes stays relatively constant. Pre-lithiation has also been successfully used to expand the voltage window and extend LIC device cyclability by regulating the anode's voltage oscillation, thereby reducing the load depth and related SEI production, volumetric expansion and ion trapping [72,81,121].

The most prevalent pre-lithiation procedure is electrochemical deposition. A closed electrical circuit develops bonding between the anode and the lithium metal [128]. This uses an electrically insulating and ionically conducting separator, similar to what is found in LIBs. Depending on the pre-doping process controllability [72,128–130], the external circuit can contain an electrical capacitor or resistor, or even a short circuit. The charging cycle can be operated with a programmable system added to the terminals [74,131]. The main drawback to this approach is extra cell assembly/disassembly procedures, where the unit ends up being assembled twice. While scientifically useful and to some extent convenient, it is not obvious how the industry can make such an approach cost-effective.

A theoretically more efficient solution could be based on chemical doping in the presence of an electrolyte [132–134]. This would occur through the direct reaction between the electrode substrate and lithium. The main advantage of this approach is its sleek simplicity and scale-up potential for industries; however, lithiation is in effect unobservable, meaning the state of charge (i.e., lithium content in the electrode), cannot be controlled or monitored until after the doping is complete. Despite this, research has been performed to alleviate this by constructing LICs with multielectrode structures to escape cell-reassembly and track the electrical signals during doping [74,135,136].

Cao and Zheng [77] demonstrated a three-electrode hybrid configuration that used stable lithium energy. Based on this theory, other types of lithium, such as lithium silicide, lithium-rich transition metal oxides, were used for different anodes (e.g., steel, silicone, etc.) [114,127,132,137]. Pre-lithiation has traditionally been done on the anode, which in turn is contradictory to how LIBs are produced; however, pre-lithiation on the cathode has been observed [115]. That would be potentially better because the system is instead constructed in a thermodynamically stable manner (which may not be the case with a symmetric unit, e.g., carbon–carbon).

During LIB production, lithium-rich ion-donating materials show a strong hysteresis during charging and discharge. This in turn causes a cycle of permanent de-lithiation during the LIBs first charge. The ions are then inserted between the main storage processes in the electrolyte and transfer back and forth during subsequent cycling. In this way materials such as Li3N [129,138] and Li6CoO4 [128,139] were able to be used as cathode additives to minimise failure. It may be possible to directly transfer this method to LICs, for example, Lukatskaya et al. [56] reported an example of the concept of a chemical additive ion source that could advance LIC technology due to its efficacy and scalability [56].

In a LIC, the activated carbon can contain sacrificial synthetic lithium salt (3,4-dihydroxybenzonitrile dilithium) [13]. This compound is irreversibly decomposed after the first cycle, with the residues dissolving in the electrolyte. It acts as a lithium-ion source inside the graphite anode without adversely impacting the electrochemical output of the

LIC. Due to the ease of converting this principle into industrial production of various LIC electrodes, the sacrificial additive method seems to have the greatest potential for practical implementations among all pre-charging approaches. In addition, the recent development of a cascade-based methodology for pre-lithiation may lead to advances in the stability of pre-lithiation of anodes.

4.1.1. Electrochemical Pre-Lithiation

Lithium metal is used as the counter-electrode for the EC method, with graphite being used as a functional electrode. Lithium ions migrate from the metal to the graphite by cycling at a fairly small current, during which the lithium electrode and graphite electrode become physically separated. Lee et al. [73] obtained pre-lithiated graphite by cycling graphite half-cells 2 times at 0.1 °C followed by a discharge of the LIC to 0.05 V during the third cycle. Similarly, by combining a mesocarbon microbead working electrode with a lithium reference electrode, Zhang et al. [140] formed pre-lithiated mesocarbon microbeads. The merit of this method is that, by setting the cut-off capacity and producing a stable SEI layer, the lithiated content can be precisely controlled. Nevertheless, the reassembly phase of the pre-lithiated anode is a time-consuming procedure unfeasible currently for use in industrial production.

4.1.2. Short-Circuit Pre-Lithiation

Often pre-lithiation of short circuits may be split into ESC (external short-circuit) and ISC (internal short-circuit) techniques. For the ESC process, a sacrificial lithium metal electrode and a targeting electrode (e.g., graphite) are separated using a porous polymer separator in a non-aqueous electrolyte and are connected to wire to naturally facilitate the penetration of lithium ions into the electrode [81,141]. Kim et al. [142] compared the different pre-lithiation approaches and showed that the ISC method was straight-forward and effective for obtaining high energy intensity DC-LICs. In the presence of an electrolyte media, the ISC technique is performed by solid metallic lithium (e.g., Li metal or Li powder) touching a carbon anode directly. Cao and Zheng [77] described a network of hard carbon/activated carbon DC-LICs by utilising a mixture of stable lithium metal powder (SLMP). Once the hard carbon—SLMP mass ratio reached between 5:1–8:1, a healthy life cycle was obtained. The extra Li powder-covered hydrogen fluoride (HF) against etching of the SEI layers. The biggest benefit of short circuit pre-lithiation is its straight-forward usability and scale-up. Despite this, the key disadvantage is that lithium utilisation cannot be precisely regulated [132].

4.1.3. Irreversible Transition Metal Oxides at the Cathode

Compared to the usage of metallic lithium, the use of permanent electrochemical lithium-transition metal oxides as a pre-lithiation agent will significantly enhance the health of LICs [63]. Usually, the chosen lithium transition metal oxides only operate on the first charge cycle to facilitate the incorporation of lithium cations into the graphite anode. Li_6CoO_4, Li_5FeO_4, Li_2CuO_2, Li_5ReO_6 and Li_2RuO_3 have been developed to be used as pre-lithiation agents [115,143–146]. Through this method, the degree of pre-lithiation can be managed by regulating the volume of lithium metal oxides in the cathode.

4.1.4. Adding Sacrificial Organic Lithium Salt

Jeżowski et al. [56] published a pre-lithiation process for sacrificial organic lithium salt, using 3,4-dihydroxybenzonitrile dilithium salt (Li_2DHBN) as a sacrificial salt in 1 M $LiPF_6$/EC–DMC. The insoluble Li_2DHBN was combined with activated carbon and released during the first charge cycle to form the soluble 3,4-dioxobenzonitrile (DOBN). The Lithium ions intercalated into the graphite to achieve pre-lithiation. Of such approaches, stable metallic lithium powder and the inclusion of permanent lithium transition metal oxides could have the most promising prospects for industrial production; however, monitoring the lithiation degree and health issues are still relevant factors. Recently, Li_3N

was employed as a sacrificial lithium compound for metal-free pre-lithiation by adding it to the electrode mixture during active material synthesis. Using this additive, stable cyclability of 91% after 10,000 cycles was observed [147].

4.2. Electrolytes

The electrolyte often serves as an integral part of the pairing LIC electrodes, greatly influencing the energy capacity, power efficiency, and cycling stability. To obtain sufficient energy and power efficiency, multiple electrolyte specifications should be met [6]: outstanding ionic conductivity; strong electrical insulation; large voltage operating window; exceptional stability; and, ideally low toxicity. Electrolytes can be classified into 4 types: aqueous electrolyte; organic electrolyte; ionic liquid electrolyte; and inorganic solid-state electrolyte. Aqueous electrolytes have high ionic conductivity and low resistance, favourable for ion transfer; however, the working voltage range is generally less than 1.2 V and is constrained by water decomposition [148]. Due to their marginal instability, good thermal, chemical and electrochemical resilience, low flammability and superior conductivity, ionic liquid-based electrolytes have been examined [149,150]; however, their use is not ideal industrially due to their high economic costs. A solid-state polymer may be an acceptable alternative electrolyte because the ionic conducting medium has electronic separators that preserve the LICs health through high cycle numbers. While in recent years solid-state polymer electrolytes have flourished and considerable improvement has been made, their ionic conductivity needs to be significantly enhanced for room temperature use.

Organic electrolytes may have the best prospects for commercially available LICs. They have a larger voltage window than aqueous electrolytes, and their operating condition is milder than that of solid-state polymer electrolytes and ionic liquid electrolytes. Organic electrolytes are commonly used in LIBs and LICs; however, their high economic cost, low potential power, low conductivity and health concerns linked to flammability, variability and toxicity are problematic [149,150]. Despite this, a modern polyethylene glycol-functionalised polysilsesquioxane has been developed for the manufacture of hybrid ionogel electrolytes for LICs [151]. This gave the electrolyte excellent thermal stability and superior ionic conductivity.

The most significant or distinct required components in electrolytes are lithium salts, solvents and additives. Solvents such as polycarbonates, ethers, ethylene carbonates, diethyl carbonates, dimethyl carbonates, propylmethyl carbonates and ethyl methyl carbonates can dissolve lithium salts and transport lithium ions [72,81,152,153]; however, the SEI shape and structure can be highly affected by the use of solvents. Additives are connected to other compounds that are applied to the electrolyte and can effectively boost efficiency. According to the different effects of the additives, they can be classified as improving ion conductivity; improving device properties (e.g., the SEI); improving low-temperature efficiency and thermal stability; preventing overloading; and, reducing electrolyte acid and water content [6,154,155].

4.3. Modelling and Simulation of LICs

LICs have a clear advantage in offering high power and energy density within a single energy storage system while maintaining a longer cycle life. Although there has been substantial research into materials and chemistries for the production of LICs, there is a requirement for research on the effect of electrode balancing and pre-lithiation on the LICs usable energy. Computational approaches have been able to provide aid in determining these effects using physics-based models based on experimental data.

When designing an LIC, many factors need to be taken into account to ensure accurate hybridisation of the LIB components with the traditional capacitor components. Using theoretical and experimental data, computational modelling has been able to be used to assist this process. Moreover, such modelling has allowed theoretical guidelines to aid the design of LICs to obtain optimal operation. Choi and Park (2014) developed a thorough theoretical analysis that aids the design of high-performance LICs, and also

developed guidelines to improve the development phase of new LICs [156]. In summary, these guidelines state that:

- battery and capacitor components must be homogeneously hybridised to operate as a single electrode (see [157] for in-depth hybridisation approaches and principles);
- the capacitor component must be highly electronically-conductive and able to store electrochemical energy in the organic electrolyte by electrostatic force, and,
- electrode material must have a high surface area to achieve high energy density and an open porous structure to achieve optimal ionic conduction.

Ghossein et al. (2018) noted that there were limitations in using LIB and supercapacitor models based on electrochemical impedance spectroscopy for LICs [158]. They stated that these models were not suitable for accurately describing the impedance of LICs at low frequencies. They concluded that this was due to the size of the pores in the cathode being identical to the anode in the LIC and supercapacitor models. Therefore, they introduced a new model that was specific to LICs and includes accurate pore sizes and distributions of the cathode. This allowed accurate modelling of impedance values at all frequencies when compared to experimental data. Madabattula el al. (2019) developed a model to study the relationship between usable energy at a variety of effective C rates and mass ratios of the electrodes in a LIC [159]. By extending the model to analyse the pre-lithiation requirement, they were able to determine the limits of pre-lithiation in Lithium Titanium oxide anodes, and how negative polarisation of the activated carbon in the cathode can improve cell capacity. In addition, in a LIC cell with a higher mass ratio, the authors were able to relate the effects of electrolyte depletion with poor power performance.

5. Knowledge and Research Gaps

Low Coulombic-related decreases in available charge in batteries are usually correlated with the irreversible and continuous creation of an SEI and certain cathode electrolyte interlay (CEI) [160,161]. This can also be the case with LICs. LICs usually have a smaller Lithium pool than traditional LIBs, have more strict criteria for reducing internal resistance losses attributable to high voltage and undergo more cycling. All three of these aspects render SEI forming a substantial challenge for LICs, and due to the wide voltage window, CEI formation can result in plugging of surface pores and, therefore, a loss of active surface area [13].

SEI products are expected to be similar to what is observed with other types of carbons used in LIBs, due to carbonate electrolyte reduction in LICs [162,163]. The electrolyte solutions solvents and salts are both thermodynamically unstable and undergo reduction on the anode during charging (when the anode is temporarily a cathode), which may operate at a potential near (or below) that of metallic lithium [164,165]. Therefore, a substance with a wide surface-to-volume ratio can induce higher irreversible losses in terms of performance [166,167]. Such reduction films may make the anode surface unreactive, protecting the electrolyte solution from further decomposition; however, any volumetric changes experienced during electrochemical cycling may weaken and fracture the SEI layer, with each cycle exposing fresh material to the electrolyte [109,168–170], creating a new layer of the SEI.

The SEI comprises primarily of electrolyte reducing materials. The instability of the SEI will inevitably trigger the LIC unit to lose overall power and fail [168,171–173]. Apart from solvent-reduction products such as Li_2CO_3 and alkyl carbonates, the SEI anode also partially consists of LiF, which is a decomposition product of the $LiPF_6$ salt but can also be produced by reaction with trace amounts of water to HF and eventually LiF [174,175]. Research on this points to radial compositional and structural gradients inside the SEI sheet, as well as complex growth-shrinking characteristics with cycling [176–179].

For a variety of carbon-supported nanomaterials (e.g., oxides and sulphides), an additional aspect relating to SEI formation in hybrid ion capacitor anode materials is linked to the cycling-induced capability gain sometimes mentioned in the literature [13]. An increase in the performance induced by cycling is not uncommon for Li-based anodes, especially for

oxides [180–184]. This phenomenon has been attributed to a contribution to load-storage through surface adsorption as a result of the extra surface area created by conversion compound cycling [184,185]; however, recent discussions have suggested this is not the case as when a carbonate electrolyte is used, the surface area of both electrodes during cycling decreases considerably [13]. They further claim that the increase in power is due to the internally parallel nanostructured anodes rather is the cycling-induced reversible forming of a polymer gel on the surface of the nanostructured electrode during lithium charging. This Faradaic cycle can be mechanistically identical to reversible and high Coulombic quality redox reactions in polymer-based electrochemical capacitors [186–188].

In LIC devices a parasitic oxidation substance (i.e., CEI), is most likely formed on the cathode. The most intuitive evidence for this oxidation layer is the commonly observed loss of the first-cycle capacity for carbon cathodes in carbonate electrolytes [98,189,190]. A secure passivation sheet could prevent any further oxidation of electrolytes on the electrode surface [191–194]. The chemical structure of the passivation substrate (e.g., size or type) on the cathodes has been observed to differ greatly from material to material [193]. Surface characterisation methods (e.g., X-ray photoelectron spectroscopy and atomic force microscopy), have been used to study passivation layers in cathodes [193–196]; however, the CEI chemistry, composition or voltage impact on its development are yet to be analysed.

In terms of its chemistry and composition, the CEI in LICs can be somewhat different from that developed on the classic LIB intercalation cathodes [13]. CEI creation is catalysed by a faradic mechanism. The sum of irreversible ability due to CEI should be directly linked to the surface area and the functionality of the surface heteroatoms, as well as the electrolyte carbonate types. Electrochemical impedance analysis has been used to observe the development and evolution of the passivation layer on a carbon cathode in an indirect way [77,197,198]; however, more in-depth analysis of the CEI in LIC devices is required, because its growth may be important to performance.

Besides the SEI and CEI materials used in LICs, carbon-based electrodes can suffer from Li plating to a greater degree than as observed in LIBs. This specifically applies to graphite, which continues to plate Lithium at various charging rates [199–206].

Nanostructured lithium titanate could greatly reduce the magnitude of lithium metal plating [121]; however, $Li_4Ti_5O_{12}$ alone is not adequately electrically conductive to reach the high levels required in LICs. The ideal method to prevent metal plating is to ensure that the anode stays far enough from 0 V vs. Li/Li^+, especially at high charging levels; however, this would require the quantification of a three-to-four-electrode cell (including reference electrodes), something that is rarely done. It should also be pointed out that the voltage swing of the individual electrodes can only be estimated from their mass-to-capacity ratio in a true two-electrode cell. This causes more problems in specifically regulating the composition of both the metal and SEI.

6. Next-Generation Lithium-Ion Capacitors

Much research in recent years has revolved around developing the electrodes used in LICs. As a result, many types have been observed to have varied performance in LIC designs. Table 3 gives an overview of the different materials researched recently.

6.1. Pseudocapacitive Oxides

Apart from carbons and titanium compounds, a variety of new anode materials is available that are either specifically designed for LICs or are added to specific systems that have original uses in LIBs. Those nanomaterials are primarily used for anodes, not for cathodes. Conversely, even the best carbon-based adsorption cathodes offer a fraction of the capacity of existing LIC anodes. Cathode work in the field is even more important, as LIB cathodes are not specifically transferable.

Because of their fast charging and discharging kinetics, the pseudocapacitive materials emerge as a significant subset of materials for LICs, together with higher gravimetric and volumetric efficiency relative to true EDLC electrodes [5]. Augustyn et al. [54] demonstrated

that the Li^+ intercalation into the orderly channels of bulk orthorhombic T-Nb_2O_5 was straight-forward, making the charging behaviour capacitor-like. These materials were referred to as pseudocapacitive intercalation compounds since, although the Li storage mechanism was not considered EDLC, EDLC-like triangular galvanostatic curves and box-like CVs were shown. Despite this, these LICs produce at fairly low power a maximum of 76 Wh kg^{-1} rendering their total effective energy around a factor of 2 lower than that for carbon-based electrodes [207].

Vanadium oxide V_2O_5 undergoes a bulk ion intercalation reaction during reversible charging, also producing a sloping profile similar to a capacitor when used as an anode. Bulk V_2O_5 can accommodate electrolyte cations (e.g., H^+, Li^+ and K^+) in aqueous systems [208–210]. They also mixed elemental analysis and X-ray diffraction to analyse the charging-storage process of V_2O_5 in an aqueous environment. They also discovered that K^+ ions inject gaps between the (00l) Miller index planes into the interlayer, and an average energy of 42 Wh kg^{-1} can be achieved with a loss of <5% over 10,000 cycles [208]. A V_2O_5-based hybrid solution can also operate in a far wider voltage window in Li+ organic systems. The authors tested the same materials V_2O_5 on CNT in lithium structures [210]. The LIC cell energy value was in the region of 40 Wh kg^{-1}, similar to aqueous electrolyte systems.

6.2. MXenes

MXene is a large family of metal carbides and carbonitrides in the two-dimensional form [211]. It has been observed that several cations (Na^+, K^+, Mg^{2+} and Al^{3+}) can intercalate reversibly through the bulk of exfoliated multilayer $T_3C_2T_x$ MXene in an aqueous electrolyte. It was also stated that Li+ ions would intercalate reversibly between layers of MXene in the organic electrolytes [212]. Because there is a significant intercalation reaction, the MXene shows pseudocapacitor CVs and galvanostatic profiles, and could therefore be grouped into the pseudocapacitive substance family [211–213]. In addition, the electrochemical analysis revealed that storage of Li was a reaction rather than a diffusion-controlled Faradic cycle, similar to the other pseudocapacitive materials.

An LIC system based on Ti_2C coupled with Kuraray YP17 activated carbon has also been proposed [214]. Here, the Ti_2C anode showed moderate working voltage with the LIC operating at an upper cut-off voltage of 3.5 V and delivering maximum energy of 50 Wh kg^{-1}. Wang et al. [214] also synthesised 3D TiC nanoparticle chains operating in a lower voltage (0.7 V vs. Li/Li^+) area. The resulting LIC system, together with a high-capacity, nitrogen-doped porous carbon cathode, provided 101.5 Wh kg^{-1} of energy and 23.4 Wh kg^{-1} energy at an intense strength of 67,500 W kg^{-1}. Additionally, Luo et al. [215] developed a CTAB-Sn pillared Ti_3C_2 MXene-based LIC system that provided energy of 105.6 Wh kg^{-1}. An important issue worth pursuing is the cyclability of these materials. Whether the existing intercalation compounds can survive such extended service and, if not, whether their structure and/or electrolyte chemistry can be tuned to enhance performance is still unknown.

6.3. Conversion Compounds

Reversible materials dependent on reaction conversion are another type that was considered pseudocapacitive and has gained popularity as a substrate for the LIC electrodes. A conversion electrode is defined initially in LIB literature as the crystalline or amorphous A_xB_y material, which then decomposes reversibly into one or two Lithium compounds after charging [216]. Some examples of the structures used for LICs are MoS2, NbN, VN, MnO, Fe_2O_3/Fe_3O_4, $NiCo_2O_4$ and various alloys. Although MoS_2 undergoes a Lithium intercalation reaction down to 1.1 V, most reversible capability stems from reversible Mo and Li_2S conversion reaction down to 0 V [217]. The reversible capability of MoS_2 is stated to be as high as 1000 $mAhg^{-1}$, which actually is higher than the theoretical figure. The discrepancy may be due to a capacitive contribution and a reversible SEI growth contribution [218]. Wang et al. [219] used MoS_2-graphene composites in LICs, using

sloping charge and discharge profiles, with the LIC delivering energy density as high as 188 Wh kg^{-1} at 200 W kg^{-1} and 45.3 Wh kg^{-1} at 40,000 W kg^{-1}. MoS_2's functional efficiency was around 600 mAh per gram and helps balance the sloping voltage plateau with fast energy delivery. The outstanding rate capability and the retention of cycling power possibly emerged in the anode from the engineered secondary carbon-based process.

6.4. Battery-Related Intercalation Ceramics

Research has been performed using ceramic LIB cathode materials coupled against carbon counter electrodes, developing a high-power LIB with a more sloping tension profile. Aravindan et al. [220] provided an excellent description of intercalation-type materials for configurations of LICs. The overwhelming majority of such architectures exhibit cyclability like batteries, lasting many thousands of cycles. For example, layered oxides, spinel oxide, olivine, NASICON and silicates are specific forms of ceramic battery cathodes used in LICs. Olivine $LiFePO_4$ is a well-established LIB commercial cathode which has also seen applications in LIC systems. During lithium intercalation/deintercalation it undergoes a two-phase reaction and shows a flat plateau at 3.4 V. Ping et al. [221] constructed a hybrid activated carbon + $LiFePO_4$ composite as the cathode and mesocarbon microbeads as the anode. The unit was cycled between 2 and 4 V with an average energy density of 69 Wh kg^{-1} and a lifespan of 100 cycles with marginal decay.

NASICON cathodes have also recently gained recognition for applications in hybrid systems. The most frequently studied NASICONs are the phases $Li_3V_2(PO_4)_3$ (LVP) and $Na_3V_2(PO_4)_3$ (NVP), with vanadium as the active metal transfer part. Satish et al. [105] incorporated an LVP-C cathode with activated carbon as an anode in a LIC device, obtaining 25 Wh kg^{-1}. For an activated carbon/LVP configuration an energy density of 28 Wh kg^{-1} was observed [222]; however, the energy efficiency becomes greatly increased (125 Wh kg^{-1} at 300 W kg^{-1}) where activated carbon is used as a cathode when LVP is the anode.

Table 3. Next-generation electrode materials for LICs.

Configuration (Anode//Cathode)	Voltage	Max Energy (Wh/kg) at Power (W/kg)	Energy (Wh/kg) at Max Power (W/kg)	Cyclability
T-Nb_2O_5-graphene//activated carbon [223]	0.8–3 V	47 at 393	15 at 18,000	93% over 2000 cycles
mesoporous Nb_2O_5–C//activated carbon [224]	1–3.5 V	74 at 120	20 at 12,137	Not reported
V_2O_5 on CNT//activated carbon [210]	0–2.7 V	40 at 210	6.9 at 6300	78% over 10,000 cycles
γ-$Li_xV_2O_5$-BM50//activated carbon [225]	0–4.5 V	54.59 at 230	Not reported	100% over 400 cycles
CTAB-Sn on Ti_3C_2 MXene//activated carbon [215]	1–4 V	105.6 at 495	45.3 at 10,800	70% over 4000 cycles
Ti_2C MXene//YP17 active carbon [212]	1–3.5 V	50 at 190	15 at 600	85% over 1000 cycles
TiC MXene//N-doped porous carbon [214]	0–4.5 V	101.5 at 450	23.4 at 67,500	82% over 5000 cycles
T-Nb_2O_5 on C//MSP-20 activated carbon [226]	1–3.5 V	63 at 70	10 at 6500	75% over 1000 cycles
Nb_2O_5-carbide-derived carbon//YP-50F AC [227]	1–2.8 V	30 at 220	18 at 5000	Not reported
Nb_2O_5–CNT//activated carbon [228]	0.5–3 V	33.5 at 82	4 at 4000	Not reported
$LiNbO_3$ on graphene aerogel//boron carbonitride nanotube [229]	1–4 V	148 at 200	69.4 at 9900	82% over 7000 cycles
MoS_2–C-RGO//PANI-derived porous carbon [219]	0–4 V	188 at 200	45.3 at 40,000	80% over 10,000 cycles
NbN//activated PANI-derived carbon [230]	0–4 V	149 at 200	5 at 45,000	95% over 15,000 cycles
VN-rGO//activated carbon [231]	0–4 V	162 at 200	64 at 10,000	83% over 1000 cycles
MnO cubes//activated carbon [232]	0–4 V	227 at 55	21 at 2952	93% over 3000 cycles
3D MnO array//activated carbon nanosheets [233]	1–4 V	184 at 83	83 at 18,000	83% over 5000 cycles
MnO nanoparticles//activated carbon [234]	0–4 V	220 at 100	35 at 2608	95.3% over 3600 cycles
MnO on C//trisodium citrate-derived carbon [235]	0–3.9 V	235 at 120	61 at 25,000	85.69% over 10,000 cycles
MnNCN//activated carbon [236]	0.1–4 V	103 at 150	22 at 4500	100% over 5000 cycles
Fe_xO on graphene//porous graphene [237]	0–3.5 V	129.6 at 19	45 at 3500	75% over 3000 cycles

Table 3. *Cont.*

Configuration (Anode//Cathode)	Voltage	Max Energy (Wh/kg) at Power (W/kg)	Energy (Wh/kg) at Max Power (W/kg)	Cyclability
Fe_2O_3//activated carbon [238]	0–3.5 V	90	Not reported	55% over 2500 cycles
Fe_3O_4 in graphene//3D graphene [239]	1–4 V	204 at 55	85 at 2650	70% over 1000 cycles
$NiCo_2O_4$//activated carbon [240]	0–4.5 V	39.4 at 120	10 at 554	100% over 2000 cycles
activated carbon//$LiMn_1/3Ni_1/3Fe_1/3O_2$–PANI [241]	0–3 V	49 at 900	19 at 3000	100% over 3000 cycles
activated carbon//$LiMn_2O_4$ [242]	0.7–3 V	45 at 60	10 at 800	Not reported
$LiNi_{0.5}Mn_{1.5}O_4$//activated carbon [243]	1.5–3.25 V	19 at 120	8 at 3500	81% over 1000 cycles
mesocarbon microbeads//$LiFePO_4$ [221]	2–4 V	69	Not reported	100% over 100 cycles
$Li_3V_2(PO_4)_3$//activated carbon [222]	0–4 V	125 at 300	65 at 6000	80% over 200 cycles
activated carbon//$Li_3V_2(PO_4)_3$ [222]	0–2.5 V	28 at 35	14 at 1500	87% over 1000 cycle
activated carbon//$Li_3V_2(PO_4)_3$ [105]	0.5–2.7 V	25 at 88	13 at 320	Not reported
Li_2MnSiO_4//activated carbon [244]	0–3 V	54 at 150	37 at 1500	85% over 1000 cycles
$LiMnBO_3$//PANI [245]	0–3 V	42 at 1500	15 at 5350	91% over 1000 cycles
$CoNiP_2O_7$//activated carbon [246]	0–4 V	116.3 at 200	66.7 at 6486.5	86.5 over 500 cycles

7. Concluding Remarks

The final power and energy of LIC systems are based primarily on design, charging-storage structure and materials used in electrodes. Overall, designs with the smoothest anode and cathode voltage, and the highest overall voltage gap are ideal. Although existing LIC designs are reasonably straightforward in material terms, the associated high-rate charging and storage mechanisms in the electrodes (especially in the anode) remain poorly understood and require further research and development. Key unresolved issues for LICs include electrode design, energy-to-power limitations, fast charging mechanisms in anodes that vary from LIB activity, SEI formation, and LIC cycling (although superior to LIBs, not yet at traditional EDLC level).

Because of SEI development, the risk of low-voltage metal plating and volume expansion, it would seem as though the anode is the bottle-neck for cycling life. Although a high-surface-area cathode may function at a voltage where a CEI is formed, the overall chemistry would be less harmful due to reduced volume expansion (CEI does not accumulate through cycling). Despite this, the creation of the CEI for LICs is almost entirely unexplored. In terms of energy density, there currently does not appear to be an ideal cathode material that could operate at comparable capacity as the anode while maintaining cycling stability. Activated carbon is stable but offers up to one-fifth of a hard carbon anode reversible capacity. More specifically, many features of carbon-based electrodes in LICs still need further investigation. One is cycling stability during high current density testing. As long-term cycling stability is essential for LICs, it appears important to evaluate the advantages of using carbon-based electrodes in LICs.

The developments in LICs are mainly due to the production of advanced carbon-based electrodes. Although significant strides have been made in the manufacture of carbon-based electrodes, more research remains to be done. The inherent electrochemical performance of the electrode materials and the growth of active materials on the electrode depends on the porous structure and surface properties of the materials used. Although many materials have been designed to either serve as the electrodes or to assist other active materials, their microstructures are disordered and random in most situations, their surface properties are not well regulated and some pores of these materials are not electrochemically available for the electrolyte, restricting their electrochemical efficiency. Furthermore, the physical properties of some materials provide additional areas of concern through their deformation during charge and discharge cycles. Although ambitious, attention should be given to the design of electrodes with precisely controllable microstructures.

Author Contributions: Conceptualization, J.J.L. and O.S.B.; methodology, J.J.L. and O.S.B.; software, J.J.L. and O.S.B.; validation, J.J.L. and O.S.B.; formal analysis, J.J.L. and O.S.B.; investigation, J.J.L. and O.S.B.; resources, J.J.L. and O.S.B.; data curation, J.J.L. and O.S.B.; writing—original draft preparation, J.J.L. and O.S.B.; writing—review and editing, J.J.L. and O.S.B.; visualization, J.J.L. and O.S.B.; supervision, J.J.L. and O.S.B.; project administration, O.S.B.; funding acquisition, O.S.B. Both authors have read and agreed to the published version of the manuscript.

Funding: This research received no external funding. The APC was funded by ENERSENSE, NTNU.

Institutional Review Board Statement: Not applicable.

Informed Consent Statement: Not applicable.

Data Availability Statement: Data is contained within the article.

Acknowledgments: Jacob J. Lamb and Odne S. Burheim acknowledge the support from the ENERSENSE research initiative at NTNU. We would also like to extend our thanks to Svein Kvernstuen (CEO, Beyonder), Kristin Skofteland (CCO, Beyonder) Fengliu Lou (R & D manager, Beyonder) and Dmytro Drobnyi (senior engineer, Beyonder).

Conflicts of Interest: The authors declare no conflict of interest.

References

1. Armaroli, N.; Balzani, V. The Future of Energy Supply: Challenges and Opportunities. *Angew. Chem. Int. Ed.* **2007**, *46*, 52–66. [CrossRef]
2. Burheim, O.S. *Engineering Energy Storage*; Elsevier BV: Amsterdam, The Netherlands, 2017.
3. Ellingsen, L.A.-W.; Singh, B.; Strømman, A.H. The size and range effect: Lifecycle greenhouse gas emissions of electric vehicles. *Environ. Res. Lett.* **2016**, *11*, 054010. [CrossRef]
4. Amatucci, G.G.; Badway, F.; du Pasquier, A.; Zheng, T. An Asymmetric Hybrid Nonaqueous Energy Storage Cell. *J. Electrochem. Soc.* **2001**, *148*, A930–A939. [CrossRef]
5. Wang, H.; Zhu, C.; Chao, D.; Yan, Q.; Fan, H.J. Nonaqueous hybrid lithium-ion and sodium-ion capacitors. *Adv. Mater.* **2017**, *29*, 1702093. [CrossRef] [PubMed]
6. Li, B.; Zheng, J.; Zhang, H.; Jin, L.; Yang, D.; Lv, H.; Shen, C.; Shellikeri, A.; Zheng, Y.; Gong, R.; et al. Electrode Materials, Electrolytes, and Challenges in Nonaqueous Lithium-Ion Capacitors. *Adv. Mater.* **2018**, *30*, e1705670. [CrossRef] [PubMed]
7. Harris, S.J.; Harris, D.J.; Li, C. Failure statistics for commercial lithium ion batteries: A study of 24 pouch cells. *J. Power Sources* **2017**, *342*, 589–597. [CrossRef]
8. Barcellona, S.; Ciccarelli, F.; Iannuzzi, D.; Piegari, L. Overview of Lithium-ion Capacitor Applications Based on Experimental Performances. *Electr. Power Compon. Syst.* **2016**, *44*, 1–13. [CrossRef]
9. Miller, J.R. Engineering electrochemical capacitor applications. *J. Power Sources* **2016**, *326*, 726–735. [CrossRef]
10. Berrueta, A.; Ursua, A.; Martin, I.S.; Eftekhari, A.; Sanchis, P. Supercapacitors: Electrical Characteristics, Modeling, Applications, and Future Trends. *IEEE Access* **2019**, *7*, 50869–50896. [CrossRef]
11. Li, H.; Lang, J.; Lei, S.; Chen, J.; Wang, K.; Liu, L.; Zhang, T.; Liu, W.; Yan, X. A High-Performance Sodium-Ion Hybrid Capacitor Constructed by Metal-Organic Framework-Derived Anode and Cathode Materials. *Adv. Funct. Mater.* **2018**, *28*, 1800757. [CrossRef]
12. Wang, C.; Xie, H.; Chen, S.; Ge, B.; Liu, D.; Wu, C.; Xu, W.; Chu, W.; Babu, G.; Ajayan, P.M.; et al. Atomic Cobalt Covalently Engineered Interlayers for Superior Lithium-Ion Storage. *Adv. Mater.* **2018**, *30*, e1802525. [CrossRef] [PubMed]
13. Ding, J.; Hu, W.; Paek, E.; Mitlin, D. Review of Hybrid Ion Capacitors: From Aqueous to Lithium to Sodium. *Chem. Rev.* **2018**, *118*, 6457–6498. [CrossRef]
14. Lu, K.; Li, D.; Gao, X.; Dai, H.; Wang, N.; Ma, H. An advanced aqueous sodium-ion supercapacitor with a manganous hexacyanoferrate cathode and a Fe_3O_4/rGO anode. *J. Mater. Chem. A* **2015**, *3*, 16013–16019. [CrossRef]
15. Ma, Y.; Chang, H.; Zhang, M.; Chen, Y. Graphene-Based Materials for Lithium-Ion Hybrid Supercapacitors. *Adv. Mater.* **2015**, *27*, 5296–5308. [CrossRef]
16. Wang, F.; Wu, X.; Yuan, X.; Liu, Z.; Zhang, Y.; Fu, L.; Zhu, Y.; Zhou, Q.; Wu, Y.; Huang, W. Latest advances in supercapacitors: From new electrode materials to novel device designs. *Chem. Soc. Rev.* **2017**, *46*, 6816–6854. [CrossRef]
17. Yu, X.Y.; Lou, X.W. Mixed Metal Sulfides for Electrochemical Energy Storage and Conversion. *Adv. Energy Mater.* **2018**, *8*, 1701592. [CrossRef]
18. Yu, G.; Xie, X.; Pan, L.; Bao, Z.; Cui, Y. Hybrid nanostructured materials for high-performance electrochemical capacitors. *Nano Energy* **2013**, *2*, 213–234. [CrossRef]
19. Shao, Y.; El-Kady, M.F.; Sun, J.; Li, Y.; Zhang, Q.; Zhu, M.; Wang, H.; Dunn, B.; Kaner, R.B. Design and Mechanisms of Asymmetric Supercapacitors. *Chem. Rev.* **2018**, *118*, 9233–9280. [CrossRef]
20. Zuo, W.; Li, R.; Zhou, C.; Li, Y.; Xia, J.; Liu, J. Battery-Supercapacitor Hybrid Devices: Recent Progress and Future Prospects. *Adv. Sci.* **2017**, *4*, 1600539. [CrossRef] [PubMed]

21. Wu, Z.; Li, L.; Yan, J.-M.; Zhang, X.-B. Materials Design and System Construction for Conventional and New-Concept Supercapacitors. *Adv. Sci.* **2017**, *4*, 1600382. [CrossRef]
22. You, P.; Kamarudin, S. Recent progress of carbonaceous materials in fuel cell applications: An overview. *Chem. Eng. J.* **2017**, *309*, 489–502. [CrossRef]
23. Sennu, P.; Aravindan, V.; Ganesan, M.; Lee, Y.-G.; Lee, Y.-S. Biomass-Derived Electrode for Next Generation Lithium-Ion Capacitors. *ChemSusChem* **2016**, *9*, 849–854. [CrossRef]
24. Wang, J.; Nie, P.; Ding, B.; Dong, S.; Hao, X.; Dou, H.; Zhang, X. Biomass derived carbon for energy storage devices. *J. Mater. Chem. A* **2017**, *5*, 2411–2428. [CrossRef]
25. Long, W.; Fang, B.; Ignaszak, A.; Wu, Z.; Wang, Y.-J.; Wilkinson, D. Biomass-derived nanostructured carbons and their composites as anode materials for lithium-ion batteries. *Chem. Soc. Rev.* **2017**, *46*, 7176–7190. [CrossRef]
26. Wang, X.; Cao, K.; Wang, Y.; Jiao, L. Controllable N-Doped $CuCo_2$ O_4 @C Film as a Self-Supported Anode for Ultrastable Sodium-Ion Batteries. *Small* **2017**, *13*, 1700873. [CrossRef]
27. Gu, H.; Zhu, Y.-E.; Yang, J.; Wei, J.; Zhou, Z. Nanomaterials and Technologies for Lithium-Ion Hybrid Supercapacitors. *ChemNanoMat* **2016**, *2*, 578–587. [CrossRef]
28. Lang, J.; Zhang, X.; Liu, B.; Wang, R.; Chen, J.; Yan, X. The roles of graphene in advanced Li-ion hybrid supercapacitors. *J. Energy Chem.* **2018**, *27*, 43–56. [CrossRef]
29. Wang, L.; Hu, X. Recent Advances in Porous Carbon Materials for Electrochemical Energy Storage. *Chem. Asian J.* **2018**, *13*, 1518–1529. [CrossRef]
30. Han, P.; Xu, G.; Han, X.; Zhao, J.; Zhou, X.; Cui, G. Lithium-Ion Capacitors in Organic Electrolyte System: Scientific Problems, Material Development, and Key Technologies. *Adv. Energy Mater.* **2018**, *8*, 1801243. [CrossRef]
31. Li, B.; Dai, F.; Xiao, Q.; Yang, L.; Shen, J.; Zhang, C.; Cai, M. Activated Carbon from Biomass Transfer for High-Energy Density Lithium-Ion Supercapacitors. *Adv. Energy Mater.* **2016**, *6*, 1600802. [CrossRef]
32. Xia, Q.; Yang, H.; Wang, M.; Yang, M.; Guo, Q.; Wan, L.; Xia, H.; Yu, Y. High Energy and High-Power Lithium-Ion Capacitors Based on Boron and Nitrogen Dual-Doped 3D Carbon Nanofibers as Both Cathode and Anode. *Adv. Energy Mater.* **2017**, *7*, 1701336. [CrossRef]
33. Sun, F.; Liu, X.; Bin Wu, H.; Wang, L.; Gao, J.; Li, H.; Lu, Y. In Situ High-Level Nitrogen Doping into Carbon Nanospheres and Boosting of Capacitive Charge Storage in Both Anode and Cathode for a High-Energy 4.5 V Full-Carbon Lithium-Ion Capacitor. *Nano Lett.* **2018**, *18*, 3368–3376. [CrossRef]
34. Yang, J.; Yu, C.; Hu, C.; Wang, M.; Li, S.; Huang, H.; Bustillo, K.; Han, X.; Zhao, C.; Guo, W.; et al. Surface-Confined Fabrication of Ultrathin Nickel Cobalt-Layered Double Hydroxide Nanosheets for High-Performance Supercapacitors. *Adv. Funct. Mater.* **2018**, *28*, 1803272. [CrossRef]
35. Martins, V.L.; Neves, H.R.; Monje, I.E.; Leite, M.M.; Oliveira, P.F.M.D.E.; Antoniassi, R.M.; Chauque, S.; Morais, W.G.; Melo, E.C.; Obana, T.T. An Overview on the Development of Electrochemical Capacitors and Batteries–Part I. *An. Acad. Bras. Cienc.* **2020**, *92*, e20200796. [CrossRef]
36. Martins, V.L.; Neves, H.R.; Monje, I.E.; Leite, M.M.; de Oliveira, P.F.; Antoniassi, R.M.; Chauque, S.; Morais, W.G.; Melo, E.C.; Obana, T.T.; et al. An Overview on the Development of Electrochemical Capacitors and Batteries—Part II. *Anais Acad. Bras. Cienc.* **2020**, *92*, e20200800. [CrossRef] [PubMed]
37. Gür, T.M. Review of electrical energy storage technologies, materials and systems: Challenges and prospects for large-scale grid storage. *Energy Environ. Sci.* **2018**, *11*, 2696–2767. [CrossRef]
38. Zubi, G.; Dufo-López, R.; Carvalho, M.; Pasaoglu, G. The lithium-ion battery: State of the art and future perspectives. *Renew. Sustain. Energy Rev.* **2018**, *89*, 292–308. [CrossRef]
39. Naoi, K. 'Nanohybrid capacitor': The next generation electrochemical capacitors. *Fuel Cells* **2010**, *10*, 825–833. [CrossRef]
40. Balamurugan, J.; Nguyen, T.T.; Aravindan, V.; Kim, N.H.; Lee, J.H. Flexible Solid-State Asymmetric Supercapacitors Based on Nitrogen-Doped Graphene Encapsulated Ternary Metal-Nitrides with Ultralong Cycle Life. *Adv. Funct. Mater.* **2018**, *28*, 1804663. [CrossRef]
41. Wang, X.; Liu, L.; Niu, Z. Carbon-based materials for lithium-ion capacitors. *Mater. Chem. Front.* **2019**, *3*, 1265–1279. [CrossRef]
42. González-Gil, A.; Palacin, R.; Batty, P. Sustainable urban rail systems: Strategies and technologies for optimal management of regenerative braking energy. *Energy Convers. Manag.* **2013**, *75*, 374–388. [CrossRef]
43. Schiele, A.; Breitung, B.; Hatsukade, T.; Berkes, B.B.; Hartmann, P.; Janek, J.; Brezesinski, T. The Critical Role of Fluoroethylene Carbonate in the Gassing of Silicon Anodes for Lithium-Ion Batteries. *ACS Energy Lett.* **2017**, *2*, 2228–2233. [CrossRef]
44. Tian, R.; Duan, H.; Guo, Y.; Li, H.; Liu, H. High-Coulombic-Efficiency Carbon/Li Clusters Composite Anode without Precycling or Prelithiation. *Small* **2018**, *14*, e1802226. [CrossRef] [PubMed]
45. Holtstiege, F.; Bärmann, P.; Nölle, R.; Winter, M.; Placke, T. Pre-Lithiation Strategies for Rechargeable Energy Storage Technologies: Concepts, Promises and Challenges. *Batteries* **2018**, *4*, 4. [CrossRef]
46. Shi, L.; Pang, C.; Chen, S.; Wang, M.; Wang, K.; Tan, Z.; Gao, P.; Ren, J.; Huang, Y.; Peng, H.; et al. Vertical Graphene Growth on SiO Microparticles for Stable Lithium-Ion Battery Anodes. *Nano Lett.* **2017**, *17*, 3681–3687. [CrossRef] [PubMed]
47. Jin, Y.; Li, S.; Kushima, A.; Zheng, X.; Sun, Y.; Xie, J.; Sun, J.; Xue, W.; Zhou, G.; Wu, J.; et al. Self-healing SEI enables full-cell cycling of a silicon-majority anode with a coulombic efficiency exceeding 99.9%. *Energy Environ. Sci.* **2017**, *10*, 580–592. [CrossRef]

48. Wang, J.; Cui, Y.; Wang, D. Design of Hollow Nanostructures for Energy Storage, Conversion and Production. *Adv. Mater.* **2019**, *31*, e1801993. [CrossRef]
49. Li, B.; Chien, S.-W.; Ge, X.; Chai, J.; Goh, X.-Y.; Nai, K.-T.; Hor, T.S.A.; Liu, Z.; Zong, Y. Ni/NiOx-decorated carbon nanofibers with enhanced oxygen evolution activity for rechargeable zinc–air batteries. *Mater. Chem. Front.* **2017**, *1*, 677–682. [CrossRef]
50. Xu, Q.; Sun, J.-K.; Li, G.; Li, J.-Y.; Yin, Y.-X.; Guo, Y.-G. Facile synthesis of a SiO x/asphalt membrane for high performance lithium-ion battery anodes. *Chem. Commun.* **2017**, *53*, 12080–12083. [CrossRef]
51. Wang, X.; Liu, Y.; Wang, Y.; Jiao, L. CuO Quantum Dots Embedded in Carbon Nanofibers as Binder-Free Anode for Sodium Ion Batteries with Enhanced Properties. *Small* **2016**, *12*, 4865–4872. [CrossRef]
52. Stoller, M.D.; Murali, S.; Quarles, N.; Zhu, Y.; Potts, J.R.; Zhu, X.; Ha, H.-W.; Ruoff, R.S. Activated graphene as a cathode material for Li-ion hybrid supercapacitors. *Phys. Chem. Chem. Phys.* **2012**, *14*, 3388. [CrossRef] [PubMed]
53. Braun, P.V.; Cook, J.B. Deterministic Design of Chemistry and Mesostructure in Li-Ion Battery Electrodes. *ACS Nano* **2018**, *12*, 3060–3064. [CrossRef]
54. Augustyn, V.; Come, J.; Lowe, M.A.; Kim, J.W.; Taberna, P.-L.; Tolbert, S.H.; Abruña, H.D.; Simon, P.; Dunn, B. High-rate electrochemical energy storage through Li+ intercalation pseudocapacitance. *Nat. Mater.* **2013**, *12*, 518–522. [CrossRef] [PubMed]
55. Rauhala, T.; Leis, J.; Kallio, T.; Vuorilehto, K. Lithium-ion capacitors using carbide-derived carbon as the positive electrode—A comparison of cells with graphite and $Li_4Ti_5O_{12}$ as the negative electrode. *J. Power Sources* **2016**, *331*, 156–166. [CrossRef]
56. Jeżowski, P.; Crosnier, O.; Deunf, E.; Poizot, P.; Béguin, F.; Brousse, T. Safe and recyclable lithium-ion capacitors using sacrificial organic lithium salt. *Nat. Mater.* **2017**, *17*, 167–173. [CrossRef]
57. Chen, K.; Cao, J.; Lu, Q.; Wang, Q.; Yao, M.; Han, M.; Niu, Z.; Chen, J. Sulfur nanoparticles encapsulated in reduced graphene oxide nanotubes for flexible lithium-sulfur batteries. *Nano Res.* **2017**, *11*, 1345–1357. [CrossRef]
58. Liu, L.; Niu, Z.; Chen, J. Unconventional supercapacitors from nanocarbon-based electrode materials to device configurations. *Chem. Soc. Rev.* **2016**, *45*, 4340–4363. [CrossRef] [PubMed]
59. Yao, F.; Pham, D.T.; Lee, Y.H. Carbon-Based Materials for Lithium-Ion Batteries, Electrochemical Capacitors, and Their Hybrid Devices. *ChemSusChem* **2015**, *8*, 2284–2311. [CrossRef] [PubMed]
60. Shehzad, K.; Xu, Y.; Gao, C.; Duan, X. Three-dimensional macro-structures of two-dimensional nanomaterials. *Chem. Soc. Rev.* **2016**, *45*, 5541–5588. [CrossRef] [PubMed]
61. Li, D.; Müller, M.B.; Gilje, S.; Kaner, R.B.; Wallace, G.G. Processable aqueous dispersions of graphene nanosheets. *Nat. Nanotechnol.* **2008**, *3*, 101–105. [CrossRef] [PubMed]
62. Yang, M.; Zhou, Z. Recent Breakthroughs in Supercapacitors Boosted by Nitrogen-Rich Porous Carbon Materials. *Adv. Sci.* **2017**, *4*, 1600408. [CrossRef]
63. Li, G.; Yang, Z.; Yin, Z.; Guo, H.; Wang, Z.; Yan, G.; Liu, Y.; Li, L.; Wang, J. Non-aqueous dual-carbon lithium-ion capacitors: A review. *J. Mater. Chem. A* **2019**, *7*, 15541–15563. [CrossRef]
64. Yang, Z.; Guo, H.; Li, X.; Wang, Z.; Wang, J.; Wang, Y.; Yan, Z.; Zhang, D. Graphitic carbon balanced between high plateau capacity and high rate capability for lithium ion capacitors. *J. Mater. Chem. A* **2017**, *5*, 15302–15309. [CrossRef]
65. Sivakkumar, S.; Milev, A.S.; Pandolfo, A. Effect of ball-milling on the rate and cycle-life performance of graphite as negative electrodes in lithium-ion capacitors. *Electrochim. Acta* **2011**, *56*, 9700–9706. [CrossRef]
66. Lim, Y.; Park, J.W.; Park, M.-S.; Byun, D.; Yu, J.; Jo, Y.N.; Kim, Y. Hard Carbon-coated Natural Graphite Electrodes for High-Energy and Power Lithium-Ion Capacitors. *Bull. Korean Chem. Soc.* **2015**, *36*, 150–155. [CrossRef]
67. Charon, E.; Rouzaud, J.-N.; Aléon, J. Graphitization at low temperatures (600–1200 °C) in the presence of iron implications in planetology. *Carbon* **2014**, *66*, 178–190. [CrossRef]
68. Dubal, D.P.; Gomez-Romero, P. All nanocarbon Li-Ion capacitor with high energy and high power density. *Mater. Today Energy* **2018**, *8*, 109–117. [CrossRef]
69. Shan, X.-Y.; Wang, Y.; Wang, D.-W.; Li, F.; Cheng, H.-M. Armoring Graphene Cathodes for High-Rate and Long-Life Lithium Ion Supercapacitors. *Adv. Energy Mater.* **2016**, *6*, 1502064. [CrossRef]
70. Yu, X.; Zhan, C.; Lv, R.; Bai, Y.; Lin, Y.; Huang, Z.-H.; Shen, W.; Qiu, X.; Kang, F. Ultrahigh-rate and high-density lithium-ion capacitors through hybriding nitrogen-enriched hierarchical porous carbon cathode with prelithiated microcrystalline graphite anode. *Nano Energy* **2015**, *15*, 43–53. [CrossRef]
71. Zhang, T.; Zhang, F.; Zhang, L.; Lu, Y.; Zhang, Y.; Yang, X.; Ma, Y.; Huang, Y. High energy density Li-ion capacitor assembled with all graphene-based electrodes. *Carbon* **2015**, *92*, 106–118. [CrossRef]
72. Khomenko, V.; Raymundo-Piñero, E.; Béguin, F. High-energy density graphite/AC capacitor in organic electrolyte. *J. Power Sources* **2008**, *177*, 643–651. [CrossRef]
73. Lee, J.H.; Shin, W.H.; Ryou, M.-H.; Jin, J.K.; Kim, J.; Choi, J.W. Functionalized Graphene for High Performance Lithium Ion Capacitors. *ChemSusChem* **2012**, *5*, 2328–2333. [CrossRef] [PubMed]
74. Kim, J.-H.; Kim, J.-S.; Lim, Y.-G.; Lee, J.-G.; Kim, Y.-J. Effect of carbon types on the electrochemical properties of negative electrodes for Li-ion capacitors. *J. Power Sources* **2011**, *196*, 10490–10495. [CrossRef]
75. Jayaraman, S.; Jain, A.; Ulaganathan, M.; Edison, E.; Srinivasan, M.; Balasubramanian, R.; Aravindan, V.; Madhavi, S. Li-ion vs. Na-ion capacitors: A performance evaluation with coconut shell derived mesoporous carbon and natural plant based hard carbon. *Chem. Eng. J.* **2017**, *316*, 506–513. [CrossRef]

76. Schroeder, M.; Winter, M.; Passerini, S.; Balducci, A. On the cycling stability of lithium-ion capacitors containing soft carbon as anodic material. *J. Power Sources* **2013**, *238*, 388–394. [CrossRef]
77. Cao, W.; Zheng, J. Li-ion capacitors with carbon cathode and hard carbon/stabilized lithium metal powder anode electrodes. *J. Power Sources* **2012**, *213*, 180–185. [CrossRef]
78. Lee, J.H.; Shin, W.H.; Lim, S.Y.; Kim, B.G.; Choi, J.W. Modified graphite and graphene electrodes for high-performance lithium-ion hybrid capacitors. *Mater. Renew. Sustain. Energy* **2014**, *3*, 1–8. [CrossRef]
79. Han, X.; Han, P.; Yao, J.; Zhang, S.; Cao, X.; Xiong, J.; Zhang, J.; Cui, G. Nitrogen-doped carbonized polyimide microsphere as a novel anode material for high performance lithium-ion capacitors. *Electrochim. Acta* **2016**, *196*, 603–610. [CrossRef]
80. Ren, J.; Su, L.; Qin, X.; Yang, M.; Wei, J.; Zhou, Z.; Shen, P. Pre-lithiated graphene nanosheets as negative electrode materials for Li-ion capacitors with high power and energy density. *J. Power Sources* **2014**, *264*, 108–113. [CrossRef]
81. Sivakkumar, S.; Pandolfo, A. Evaluation of lithium-ion capacitors assembled with pre-lithiated graphite anode and activated carbon cathode. *Electrochim. Acta* **2012**, *65*, 280–287. [CrossRef]
82. Jiang, J.; Nie, P.; Ding, B.; Zhang, Y.; Xu, G.; Wu, L.; Dou, H.; Zhang, X. Highly stable lithium-ion capacitor enabled by hierarchical polyimide derived carbon microspheres combined with 3D current collectors. *J. Mater. Chem. A* **2017**, *5*, 23283–23291. [CrossRef]
83. Zhang, J.; Liu, X.; Wang, J.; Shi, J.; Shi, Z. Different types of pre-lithiated hard carbon as negative electrode material for lithium-ion capacitors. *Electrochim. Acta* **2016**, *187*, 134–142. [CrossRef]
84. Sun, X.; Zhang, X.; Liu, W.; Wang, K.; Li, C.; Li, Z.; Ma, Y. Electrochemical performances and capacity fading behaviors of activated carbon/hard carbon lithium-ion capacitor. *Electrochim. Acta* **2017**, *235*, 158–166. [CrossRef]
85. Ahn, W.; Lee, D.U.; Li, G.; Feng, K.; Wang, X.; Yu, A.; Lui, G.; Chen, Z. Highly Oriented Graphene Sponge Electrode for Ultra High Energy Density Lithium-Ion Hybrid Capacitors. *ACS Appl. Mater. Interfaces* **2016**, *8*, 25297–25305. [CrossRef] [PubMed]
86. Phattharasupakun, N.; Wutthiprom, J.; Suktha, P.; Ma, N.; Sawangphruk, M. Enhancing the Charge Storage Capacity of Lithium-Ion Capacitors Using Nitrogen-Doped Reduced Graphene Oxide Aerogel as a Negative Electrode: A Hydrodynamic Rotating Disk Electrode Investigation. *J. Electrochem. Soc.* **2018**, *165*, A609–A617. [CrossRef]
87. Kim, H.; Cho, M.-Y.; Kim, M.-H.; Park, K.-Y.; Gwon, H.; Lee, Y.; Roh, K.C.; Kang, K. A Novel High-Energy Hybrid Supercapacitor with an Anatase TiO_2-Reduced Graphene Oxide Anode and an Activated Carbon Cathode. *Adv. Energy Mater.* **2013**, *3*, 1500–1506. [CrossRef]
88. Song, H.; Fu, J.; Ding, K.; Huang, C.; Wu, K.; Zhang, X.; Gao, B.; Huo, K.; Peng, X.; Chu, P.K. Flexible Nb_2O_5 nanowires/graphene film electrode for high-performance hybrid Li-ion supercapacitors. *J. Power Sources* **2016**, *328*, 599–606. [CrossRef]
89. Zhang, C.; Beidaghi, M.; Naguib, M.; Lukatskaya, M.R.; Zhao, M.-Q.; Dyatkin, B.; Cook, K.M.; Kim, S.J.; Eng, B.; Xiao, X.; et al. Synthesis and Charge Storage Properties of Hierarchical Niobium Pentoxide/Carbon/Niobium Carbide (MXene) Hybrid Materials. *Chem. Mater.* **2016**, *28*, 3937–3943. [CrossRef]
90. Deng, B.; Lei, T.; Zhu, W.; Xiao, L.; Liu, J. In-Plane Assembled Orthorhombic Nb_2 O_5 Nanorod Films with High-Rate Li+ Intercalation for High-Performance Flexible Li-Ion Capacitors. *Adv. Funct. Mater.* **2018**, *28*, 1704330. [CrossRef]
91. Kim, E.; Kim, H.; Park, B.-J.; Han, Y.-H.; Park, J.H.; Cho, J.; Lee, S.-S.; Son, J.G. Etching-Assisted Crumpled Graphene Wrapped Spiky Iron Oxide Particles for High-Performance Li-Ion Hybrid Supercapacitor. *Small* **2018**, *14*, e1704209. [CrossRef]
92. Liu, H.; Liu, X.; Wang, S.; Liu, H.-K.; Li, L. Transition metal based battery-type electrodes in hybrid supercapacitors: A review. *Energy Storage Mater.* **2020**, *28*, 122–145. [CrossRef]
93. Wang, F.; Wang, C.; Zhao, Y.; Liu, Z.; Chang, Z.; Fu, L.; Zhu, Y.; Wu, Y.; Zhao, D. A Quasi-Solid-State Li-Ion Capacitor Based on Porous TiO_2Hollow Microspheres Wrapped with Graphene Nanosheets. *Small* **2016**, *12*, 6207–6213. [CrossRef]
94. Yang, C.; Lan, J.-L.; Liu, W.-X.; Liu, Y.; Yu, Y.-H.; Yang, X.-P. High-Performance Li-Ion Capacitor Based on an Activated Carbon Cathode and Well-Dispersed Ultrafine TiO_2 Nanoparticles Embedded in Mesoporous Carbon Nanofibers Anode. *ACS Appl. Mater. Interfaces* **2017**, *9*, 18710–18719. [CrossRef]
95. Wang, H.; Guan, C.; Wang, X.; Fan, H.J. A High Energy and Power Li-Ion Capacitor Based on a TiO_2Nanobelt Array Anode and a Graphene Hydrogel Cathode. *Small* **2015**, *11*, 1470–1477. [CrossRef]
96. Chen, Z.; Yuan, Y.; Zhou, H.; Wang, X.; Gan, Z.; Wang, F.; Lu, Y. 3D Nanocomposite Architectures from Carbon-Nanotube-Threaded Nanocrystals for High-Performance Electrochemical Energy Storage. *Adv. Mater.* **2014**, *26*, 339–345. [CrossRef]
97. Liu, Y.; Wang, W.; Chen, J.; Li, X.; Cheng, Q.; Wang, G. Fabrication of porous lithium titanate self-supporting anode for high performance lithium-ion capacitor. *J. Energy Chem.* **2020**, *50*, 344–350. [CrossRef]
98. Aravindan, V.; Mhamane, D.; Ling, W.C.; Ogale, S.; Madhavi, S. Nonaqueous Lithium-Ion Capacitors with High Energy Densities using Trigol-Reduced Graphene Oxide Nanosheets as Cathode-Active Material. *ChemSusChem* **2013**, *6*, 2240–2244. [CrossRef]
99. Naoi, K.; Ishimoto, S.; Isobe, Y.; Aoyagi, S. High-rate nano-crystalline $Li_4Ti_5O_{12}$ attached on carbon nanofibers for hybrid supercapacitors. *J. Power Sources* **2010**, *195*, 6250–6254. [CrossRef]
100. Gao, L.; Huang, D.; Shen, Y.; Wang, M. Rutile-TiO_2 decorated Li_4 Ti_5 O_{12} nanosheet arrays with 3D interconnected architecture as anodes for high performance hybrid supercapacitors. *J. Mater. Chem. A* **2015**, *3*, 23570–23576. [CrossRef]
101. Gokhale, R.; Aravindan, V.; Yadav, P.; Jain, S.; Phase, D.; Madhavi, S.; Ogale, S. Oligomer-salt derived 3D, heavily nitrogen doped, porous carbon for Li-ion hybrid electrochemical capacitors application. *Carbon* **2014**, *80*, 462–471. [CrossRef]
102. Leng, K.; Zhang, F.; Zhang, L.; Zhang, T.; Wu, Y.; Lu, Y.; Huang, Y.; Chen, Y. Graphene-based Li-ion hybrid supercapacitors with ultrahigh performance. *Nano Res.* **2013**, *6*, 581–592. [CrossRef]

103. Deng, S.; Li, J.; Sun, S.; Wang, H.; Liu, J.; Yan, H. Synthesis and electrochemical properties of $Li_4Ti_5O_{12}$ spheres and its application for hybrid supercapacitors. *Electrochim. Acta* **2014**, *146*, 37–43. [CrossRef]
104. Kim, H.; Park, K.-Y.; Cho, M.-Y.; Kim, M.-H.; Hong, J.; Jung, S.-K.; Roh, K.C.; Kang, K. High-Performance Hybrid Supercapacitor Based on Graphene-Wrapped $Li_4Ti_5O_{12}$ and Activated Carbon. *ChemElectroChem* **2013**, *1*, 125–130. [CrossRef]
105. Satish, R.; Aravindan, V.; Ling, W.C.; Madhavi, S. Carbon-coated Li_3V_2 $(PO_4)_3$ as insertion type electrode for lithium-ion hybrid electrochemical capacitors: An evaluation of anode and cathodic performance. *J. Power Sources* **2015**, *281*, 310–317. [CrossRef]
106. Aravindan, V.; Chuiling, W.; Reddy, M.V.; Rao, G.V.S.; Chowdari, B.V.R.; Madhavi, S. Carbon coated nano-$LiTi_2$ $(PO_4)_3$ electrodes for non-aqueous hybrid supercapacitors. *Phys. Chem. Chem. Phys.* **2012**, *14*, 5808–5814. [CrossRef] [PubMed]
107. Jiao, X.; Hao, Q.; Xia, X.; Yao, D.; Ouyang, Y.; Lei, W. Boosting long-cycle-life energy storage with holey graphene supported $TiNb_2O_7$ network nanostructure for lithium-ion hybrid supercapacitors. *J. Power Sources* **2018**, *403*, 66–75. [CrossRef]
108. Shen, T.; Yao, Z.; Xia, X.; Wang, X.; Gu, C.; Tu, J. Rationally Designed Silicon Nanostructures as Anode Material for Lithium-Ion Batteries. *Adv. Eng. Mater.* **2018**, *20*, 1700591. [CrossRef]
109. Chan, C.K.; Peng, H.; Liu, G.; McIlwrath, K.; Zhang, X.F.; Huggins, R.A.; Cui, Y. High-performance lithium battery anodes using silicon nanowires. *Nat. Nanotechnol.* **2007**, *3*, 31–35. [CrossRef]
110. An, Y.-B.; Chen, S.; Zou, M.-M.; Geng, L.-B.; Sun, X.-Z.; Zhang, X.; Wang, K.; Ma, Y.-W. Improving anode performances of lithium-ion capacitors employing carbon–Si composites. *Rare Met.* **2019**, *38*, 1113–1123. [CrossRef]
111. Wang, B.; Li, X.; Luo, B.; Xinghao, Z.; Zhou, M.; Zhang, X.; Fan, Z.; Zhi, L. Approaching the Downsizing Limit of Silicon for Surface-Controlled Lithium Storage. *Adv. Mater.* **2015**, *27*, 1526–1532. [CrossRef] [PubMed]
112. Feng, K.; Li, M.; Liu, W.; Kashkooli, A.G.; Xiao, X.; Cai, M.; Chen, Z. Silicon-Based Anodes for Lithium-Ion Batteries: From Fundamentals to Practical Applications. *Small* **2018**, *14*, 1702737. [CrossRef]
113. Yi, R.; Chen, S.; Song, J.; Gordin, M.L.; Manivannan, A.; Wang, D. High-Performance Hybrid Supercapacitor Enabled by a High-Rate Si-based Anode. *Adv. Funct. Mater.* **2014**, *24*, 7433–7439. [CrossRef]
114. Zhao, J.; Lu, Z.; Liu, N.; Lee, H.-W.; McDowell, M.T.; Cui, Y. Dry-air-stable lithium silicide–lithium oxide core–shell nanoparticles as high-capacity prelithiation reagents. *Nat. Commun.* **2014**, *5*, 5088. [CrossRef] [PubMed]
115. Zhang, S.S. Eliminating pre-lithiation step for making high energy density hybrid Li-ion capacitor. *J. Power Sources* **2017**, *343*, 322–328. [CrossRef]
116. Zhou, L.; Zhang, K.; Hu, Z.; Tao, Z.; Mai, L.; Kang, Y.-M.; Chou, S.-L.; Chen, J. Recent Developments on and Prospects for Electrode Materials with Hierarchical Structures for Lithium-Ion Batteries. *Adv. Energy Mater.* **2018**, *8*, 1701415. [CrossRef]
117. Xu, Y.; Liu, Q.; Zhu, Y.; Liu, Y.; Langrock, A.; Zachariah, M.R.; Wang, C. Uniform Nano-Sn/C Composite Anodes for Lithium-Ion Batteries. *Nano Lett.* **2013**, *13*, 470–474. [CrossRef] [PubMed]
118. Derrien, G.; Hassoun, J.; Panero, S.; Scrosati, B. Nanostructured Sn–C Composite as an Advanced Anode Material in High-Performance Lithium-Ion Batteries. *Adv. Mater.* **2007**, *19*, 2336–2340. [CrossRef]
119. Banerjee, A.; Upadhyay, K.K.; Puthusseri, D.; Aravindan, V.; Madhavi, S.; Ogale, S. MOF-derived crumpled-sheet-assembled perforated carbon cuboids as highly effective cathode active materials for ultra-high energy density Li-ion hybrid electrochemical capacitors (Li-HECs). *Nanoscale* **2014**, *6*, 4387–4394. [CrossRef]
120. Cai, M.; Sun, X.; Chen, W.; Qiu, Z.; Chen, L.; Li, X.; Wang, J.; Liu, Z.; Nie, Y. Performance of lithium-ion capacitors using pre-lithiated multiwalled carbon nanotubes/graphite composite as negative electrode. *J. Mater. Sci.* **2017**, *53*, 749–758. [CrossRef]
121. Naoi, K.; Ishimoto, S.; Miyamoto, J.-I.; Naoi, W. Second generation 'nanohybrid supercapacitor': Evolution of capacitive energy storage devices. *Energy Environ. Sci.* **2012**, *5*, 9363–9373. [CrossRef]
122. Han, P.; Ma, W.; Pang, S.; Kong, Q.; Yao, J.; Bi, C.; Cui, G. Graphene decorated with molybdenum dioxide nanoparticles for use in high energy lithium-ion capacitors with an organic electrolyte. *J. Mater. Chem. A* **2013**, *1*, 5949–5954. [CrossRef]
123. Arnaiz, M.; Shanmukaraj, D.; Carriazo, D.; Bhattacharjya, D.; Villaverde, A.; Armand, M.; Ajuria, J. A transversal low-cost pre-metallation strategy enabling ultrafast and stable metal ion capacitor technologies. *Energy Environ. Sci.* **2020**, *13*, 2441–2449. [CrossRef]
124. Jin, L.; Shen, C.; Shellikeri, A.; Wu, Q.; Zheng, J.; Andrei, P.; Zhang, J.-G.; Zheng, J.P. Progress and perspectives on pre-lithiation technologies for lithium-ion capacitors. *Energy Environ. Sci.* **2020**, *13*, 2341–2362. [CrossRef]
125. Lotfabad, E.M.; Kalisvaart, P.; Kohandehghan, A.; Karpuzov, D.; Mitlin, D. Origin of non-SEI related coulombic efficiency loss in carbons tested against Na and Li. *J. Mater. Chem. A* **2014**, *2*, 19685–19695. [CrossRef]
126. Ding, J.; Wang, H.; Li, Z.; Cui, K.; Karpuzov, D.; Tan, X.; Kohandehghan, A.; Mitlin, D. Peanut shell hybrid sodium ion capacitor with extreme energy–power rivals lithium-ion capacitors. *Energy Environ. Sci.* **2015**, *8*, 941–955. [CrossRef]
127. Jarvis, C.; Lain, M.; Yakovleva, M.; Gao, Y. A prelithiated carbon anode for lithium-ion battery applications. *J. Power Sources* **2006**, *162*, 800–802. [CrossRef]
128. Park, H.; Kim, M.; Xu, F.; Jung, C.; Hong, S.M.; Koo, C.M. In situ synchrotron wide-angle X-ray scattering study on rapid lithiation of graphite anode via direct contact method for Li-ion capacitors. *J. Power Sources* **2015**, *283*, 68–73. [CrossRef]
129. Liu, X.; Jung, H.-G.; Kim, S.-O.; Choi, H.-S.; Lee, S.; Moon, J.H.; Lee, J.K. Silicon/copper dome-patterned electrodes for high-performance hybrid supercapacitors. *Sci. Rep.* **2013**, *3*, 3183. [CrossRef] [PubMed]
130. Elazari, R.; Salitra, G.; Gershinsky, G.; Garsuch, A.; Panchenko, A.; Aurbach, D. Li Ion Cells Comprising Lithiated Columnar Silicon Film Anodes, TiS_2 Cathodes and Fluoroethyene Carbonate (FEC) as a Critically Important Component. *J. Electrochem. Soc.* **2012**, *159*, A1440–A1445. [CrossRef]

131. Woo, S.H.; Park, Y.; Choi, W.Y.; Choi, N.-S.; Nam, S.; Park, B.; Lee, K.T. Trigonal $Na_4Ti_5O_{12}$ Phase as an Intercalation Host for Rechargeable Batteries. *J. Electrochem. Soc.* **2012**, *159*, A2016–A2023. [CrossRef]
132. Park, M.-S.; Lim, Y.-G.; Kim, J.-H.; Kim, Y.-J.; Cho, J.; Kim, J.-S. A Novel Lithium-Doping Approach for an Advanced Lithium-Ion Capacitor. *Adv. Energy Mater.* **2011**, *1*, 1002–1006. [CrossRef]
133. Seong, I.W.; Kim, K.T.; Yoon, W.Y. Electrochemical behavior of a lithium-pre-doped carbon-coated silicon monoxide anode cell. *J. Power Sources* **2009**, *189*, 511–514. [CrossRef]
134. Longoni, G.; Fiore, M.; Kim, J.-H.; Jung, Y.H.; Kim, D.K.; Mari, C.M.; Ruffo, R. Co_3O_4 negative electrode material for rechargeable sodium ion batteries: An investigation of conversion reaction mechanism and morphology-performances correlations. *J. Power Sources* **2016**, *332*, 42–50. [CrossRef]
135. Sun, X.; Zhang, X.; Zhang, H.; Xu, N.; Wang, K.; Ma, Y. High performance lithium-ion hybrid capacitors with pre-lithiated hard carbon anodes and bifunctional cathode electrodes. *J. Power Sources* **2014**, *270*, 318–325. [CrossRef]
136. Xu, N.; Sun, X.; Zhang, X.; Wang, K.; Ma, Y. A two-step method for preparing $Li_4Ti_5O_{12}$–graphene as an anode material for lithium-ion hybrid capacitors. *RSC Adv.* **2015**, *5*, 94361–94368. [CrossRef]
137. Wang, Z.; Fu, Y.; Zhang, Z.; Yuan, S.; Amine, K.; Battaglia, V.; Liu, G. Application of Stabilized Lithium Metal Powder (SLMP®) in graphite anode—A high efficient prelithiation method for lithium-ion batteries. *J. Power Sources* **2014**, *260*, 57–61. [CrossRef]
138. Park, K.; Yu, B.-C.; Goodenough, J.B. Li_3N as a Cathode Additive for High-Energy-Density Lithium-Ion Batteries. *Adv. Energy Mater.* **2016**, *6*, 1502534. [CrossRef]
139. Noh, M.; Cho, J. Role of Li6CoO4Cathode Additive in Li-Ion Cells Containing Low Coulombic Efficiency Anode Material. *J. Electrochem. Soc.* **2012**, *159*, A1329–A1334. [CrossRef]
140. Zhang, J.; Wu, H.; Wang, J.; Shi, J.; Shi, Z. Pre-lithiation design and lithium-ion intercalation plateaus utilization of mesocarbon microbeads anode for lithium-ion capacitors. *Electrochim. Acta* **2015**, *182*, 156–164. [CrossRef]
141. Gourdin, G.; Smith, P.H.; Jiang, T.; Tran, T.N.; Qu, D. Lithiation of amorphous carbon negative electrode for Li ion capacitor. *J. Electroanal. Chem.* **2013**, *688*, 103–112. [CrossRef]
142. Kim, M.; Xu, F.; Lee, J.H.; Jung, C.; Hong, S.M.; Zhang, Q.M.; Koo, C.M. A fast and efficient pre-doping approach to high energy density lithium-ion hybrid capacitors. *J. Mater. Chem. A* **2014**, *2*, 10029–10033. [CrossRef]
143. Park, M.-S.; Lim, Y.-G.; Hwang, S.M.; Kim, J.H.; Kim, J.-S.; Dou, S.X.; Cho, J.; Kim, Y.-J. Scalable Integration of Li_5FeO_4 towards Robust, High-Performance Lithium-Ion Hybrid Capacitors. *ChemSusChem* **2014**, *7*, 3138–3144. [CrossRef] [PubMed]
144. Lim, Y.-G.; Kim, D.; Lim, J.-M.; Kim, J.-S.; Yu, J.-S.; Kim, Y.-J.; Byun, D.; Cho, M.; Cho, K.; Park, M.-S. Anti-fluorite Li_6CoO_4 as an alternative lithium source for lithium-ion capacitors: An experimental and first principles study. *J. Mater. Chem. A* **2015**, *3*, 12377–12385. [CrossRef]
145. Park, M.-S.; Lim, Y.-G.; Park, J.-W.; Kim, J.-S.; Lee, J.-W.; Kim, J.H.; Dou, S.X.; Kim, Y.-J. Li_2RuO_3 as an Additive for High-Energy Lithium-Ion Capacitors. *J. Phys. Chem. C* **2013**, *117*, 11471–11478. [CrossRef]
146. Jeżowski, P.; Fic, K.; Crosnier, O.; Brousse, T.; Béguin, F. Lithium rhenium(vii) oxide as a novel material for graphite pre-lithiation in high performance lithium-ion capacitors. *J. Mater. Chem. A* **2016**, *4*, 12609–12615. [CrossRef]
147. Sun, C.; Zhang, X.; Li, C.; Wang, K.; Sun, X.; Ma, Y. High-efficiency sacrificial prelithiation of lithium-ion capacitors with superior energy-storage performance. *Energy Storage Mater.* **2020**, *24*, 160–166. [CrossRef]
148. Wang, Y.; Song, Y.; Xia, Y. Electrochemical capacitors: Mechanism, materials, systems, characterization and applications. *Chem. Soc. Rev.* **2016**, *45*, 5925–5950. [CrossRef] [PubMed]
149. Zhong, C.; Deng, Y.; Hu, W.; Qiao, J.; Zhang, L.; Zhang, J. A review of electrolyte materials and compositions for electrochemical supercapacitors. *Chem. Soc. Rev.* **2015**, *44*, 7484–7539. [CrossRef] [PubMed]
150. Na, W.; Lee, A.S.; Lee, J.H.; Hong, S.M.; Kim, E.; Koo, C.M. Hybrid ionogel electrolytes with POSS epoxy networks for high temperature lithium-ion capacitors. *Solid State Ionics* **2017**, *309*, 27–32. [CrossRef]
151. Na, W.; Lee, A.S.; Lee, J.H.; Hwang, S.S.; Hong, S.M.; Kim, E.; Koo, C.M. Lithium-ion capacitors fabricated with polyethylene oxide-functionalized polysilsesquioxane hybrid ionogel electrolytes. *Electrochim. Acta* **2016**, *188*, 582–588. [CrossRef]
152. Aida, T.; Murayama, I.; Yamada, K.; Morita, M. Analyses of Capacity Loss and Improvement of Cycle Performance for a High-Voltage Hybrid Electrochemical Capacitor. *J. Electrochem. Soc.* **2007**, *154*, A798. [CrossRef]
153. Aida, T.; Yamada, K.; Morita, M. An Advanced Hybrid Electrochemical Capacitor That Uses a Wide Potential Range at the Positive Electrode. *Electrochem. Solid-State Lett.* **2006**, *9*, A534–A536. [CrossRef]
154. Nakajima, T.; Dan, K.-I.; Koh, M.; Ino, T.; Shimizu, T. Effect of addition of fluoroethers to organic solvents for lithium-ion secondary batteries. *J. Fluor. Chem.* **2001**, *111*, 167–174. [CrossRef]
155. Zhang, S.; Xu, K.; Jow, T. Tris(2,2,2-trifluoroethyl) phosphite as a co-solvent for nonflammable electrolytes in Li-ion batteries. *J. Power Sources* **2003**, *113*, 166–172. [CrossRef]
156. Choi, H.S.; Park, C.R. Theoretical guidelines to designing high performance energy storage device based on hybridization of lithium-ion battery and supercapacitor. *J. Power Sources* **2014**, *259*, 1–14. [CrossRef]
157. Cericola, D.; Kötz, R. Hybridization of rechargeable batteries and electrochemical capacitors: Principles and limits. *Electrochim. Acta* **2012**, *72*, 1–17. [CrossRef]
158. El Ghossein, N.; Sari, A.; Venet, P.; Sarı, A. A Lithium-Ion Capacitor electrical model considering pore size dispersion. In Proceedings of the 2018 IEEE International Conference on Industrial Technology (ICIT), Lyon, France, 20–22 February 2018; IEEE: Piscataway, NJ, USA, 2018; pp. 1738–1742.

159. Madabattula, G.; Wu, B.; Marinescu, M.; Offer, G. How to Design Lithium-Ion Capacitors: Modelling, Mass Ratio of Electrodes and Pre-lithiation. *J. Electrochem. Soc.* **2020**, *167*, 013527. [CrossRef]
160. Xu, K. Nonaqueous Liquid Electrolytes for Lithium-Based Rechargeable Batteries. *Chem. Rev.* **2004**, *104*, 4303–4418. [CrossRef]
161. Broussely, M.; Biensan, P.; Bonhomme, F.; Blanchard, P.; Herreyre, S.; Nechev, K.; Staniewicz, R. Main aging mechanisms in Li ion batteries. *J. Power Sources* **2005**, *146*, 90–96. [CrossRef]
162. Komaba, S.; Murata, W.; Ishikawa, T.; Yabuuchi, N.; Ozeki, T.; Nakayama, T.; Ogata, A.; Gotoh, K.; Fujiwara, K. Electrochemical Na Insertion and Solid Electrolyte Interphase for Hard-Carbon Electrodes and Application to Na-Ion Batteries. *Adv. Funct. Mater.* **2011**, *21*, 3859–3867. [CrossRef]
163. Aurbach, D.; Markovsky, B.; Weissman, I.; Levi, E.; Ein-Eli, Y. On the correlation between surface chemistry and performance of graphite negative electrodes for Li ion batteries. *Electrochim. Acta* **1999**, *45*, 67–86. [CrossRef]
164. Aurbach, D.; Markovsky, B.; Levi, M.; Levi, E.; Schechter, A.; Moshkovich, M.; Cohen, Y. New insights into the interactions between electrode materials and electrolyte solutions for advanced nonaqueous batteries. *J. Power Sources* **1999**, *81*, 95–111. [CrossRef]
165. Etacheri, V.; Geiger, U.; Gofer, Y.; Roberts, G.A.; Stefan, I.C.; Fasching, R.; Aurbach, D. Exceptional Electrochemical Performance of Si-Nanowires in 1,3-Dioxolane Solutions: A Surface Chemical Investigation. *Langmuir* **2012**, *28*, 6175–6184. [CrossRef]
166. Forney, M.W.; Ganter, M.J.; Staub, J.W.; Ridgley, R.D.; Landi, B.J. Prelithiation of Silicon–Carbon Nanotube Anodes for Lithium-Ion Batteries by Stabilized Lithium Metal Powder (SLMP). *Nano Lett.* **2013**, *13*, 4158–4163. [CrossRef] [PubMed]
167. Dileo, R.A.; Ganter, M.J.; Thone, M.N.; Forney, M.W.; Staub, J.W.; Rogers, R.E.; Landi, B.J. Balanced approach to safety of high capacity silicon–germanium–carbon nanotube free-standing lithium ion battery anodes. *Nano Energy* **2013**, *2*, 268–275. [CrossRef]
168. Lotfabad, E.M.; Kalisvaart, P.; Cui, K.; Kohandehghan, A.; Kupsta, M.; Olsen, B.; Mitlin, D. ALD TiO_2 coated silicon nanowires for lithium-ion battery anodes with enhanced cycling stability and coulombic efficiency. *Phys. Chem. Chem. Phys.* **2013**, *15*, 13646–13657. [CrossRef] [PubMed]
169. Kohandehghan, A.; Kalisvaart, P.; Cui, K.; Kupsta, M.; Memarzadeh, E.; Mitlin, D. Silicon nanowire lithium-ion battery anodes with ALD deposited TiN coatings demonstrate a major improvement in cycling performance. *J. Mater. Chem. A* **2013**, *1*, 12850–12861. [CrossRef]
170. Kohandehghan, A.; Cui, K.; Kupsta, M.; Memarzadeh, E.; Kalisvaart, P.; Mitlin, D. Nanometer-scale Sn coatings improve the performance of silicon nanowire LIB anodes. *J. Mater. Chem. A* **2014**, *2*, 11261–11279. [CrossRef]
171. Xu, K.; von Cresce, A. Interfacing electrolytes with electrodes in Li ion batteries. *J. Mater. Chem.* **2011**, *21*, 9849–9864. [CrossRef]
172. Liu, D.; Cao, G. Engineering nanostructured electrodes and fabrication of film electrodes for efficient lithium-ion intercalation. *Energy Environ. Sci.* **2010**, *3*, 1218–1237. [CrossRef]
173. Karki, K.; Zhu, Y.; Liu, Y.; Sun, C.-F.; Hu, L.; Wang, Y.; Wang, C.; Cumings, J. Hoop-Strong Nanotubes for Battery Electrodes. *ACS Nano* **2013**, *7*, 8295–8302. [CrossRef]
174. Chan, C.K.; Ruffo, R.; Hong, S.S.; Cui, Y. Surface chemistry and morphology of the solid electrolyte interphase on silicon nanowire lithium-ion battery anodes. *J. Power Sources* **2009**, *189*, 1132–1140. [CrossRef]
175. Xiao, X.; Lu, P.; Ahn, D. Ultrathin Multifunctional Oxide Coatings for Lithium-Ion Batteries. *Adv. Mater.* **2011**, *23*, 3911–3915. [CrossRef]
176. Ramos-Sanchez, G.; Soto, F.A.; de la Hoz, J.M.M.; Liu, Z.; Mukherjee, P.P.; El-Mellouhi, F.; Seminario, J.M.; Balbuena, P.B. Computational Studies of Interfacial Reactions at Anode Materials: Initial Stages of the Solid-Electrolyte-Interphase Layer Formation. *J. Electrochem. Energy Convers. Storage* **2016**, *13*, 031002. [CrossRef]
177. Takenaka, N.; Suzuki, Y.; Sakai, H.; Nagaoka, M. On Electrolyte-Dependent Formation of Solid Electrolyte Interphase Film in Lithium-Ion Batteries: Strong Sensitivity to Small Structural Difference of Electrolyte Molecules. *J. Phys. Chem. C* **2014**, *118*, 10874–10882. [CrossRef]
178. Edström, K.; Herstedt, M.; Abraham, D.P. A new look at the solid electrolyte interphase on graphite anodes in Li-ion batteries. *J. Power Sources* **2006**, *153*, 380–384. [CrossRef]
179. Nie, M.; Abraham, D.P.; Chen, Y.; Bose, A.; Lucht, B.L. Silicon Solid Electrolyte Interphase (SEI) of Lithium-Ion Battery Characterized by Microscopy and Spectroscopy. *J. Phys. Chem. C* **2013**, *117*, 13403–13412. [CrossRef]
180. Li, Z.; Ding, J.; Wang, H.; Cui, K.; Stephenson, T.; Karpuzov, D.; Mitlin, D. High rate SnO_2–Graphene Dual Aerogel anodes and their kinetics of lithiation and sodiation. *Nano Energy* **2015**, *15*, 369–378. [CrossRef]
181. Xu, Z.; Wang, H.; Li, Z.; Kohandehghan, A.; Ding, J.; Chen, J.; Cui, K.; Mitlin, D. Sulfur Refines MoO_2 Distribution Enabling Improved Lithium-Ion Battery Performance. *J. Phys. Chem. C* **2014**, *118*, 18387–18396. [CrossRef]
182. Shi, Y.; Guo, B.; Corr, S.A.; Shi, Q.; Hu, Y.-S.; Heier, K.R.; Chen, L.; Seshadri, R.; Stucky, G.D. Ordered Mesoporous Metallic MoO_2 Materials with Highly Reversible Lithium Storage Capacity. *Nano Lett.* **2009**, *9*, 4215–4220. [CrossRef]
183. Sun, Y.; Hu, X.; Luo, W.; Huang, Y. Self-Assembled Hierarchical MoO_2/Graphene Nanoarchitectures and Their Application as a High-Performance Anode Material for Lithium-Ion Batteries. *ACS Nano* **2011**, *5*, 7100–7107. [CrossRef]
184. Guo, B.; Fang, X.; Li, B.; Shi, Y.; Ouyang, C.; Hu, Y.-S.; Wang, Z.; Stucky, G.D.; Chen, L. Synthesis and Lithium Storage Mechanism of Ultrafine MoO_2 Nanorods. *Chem. Mater.* **2012**, *24*, 457–463. [CrossRef]
185. Yang, L.; Gao, Q.; Zhang, Y.; Tang, Y.; Wu, Y. Tremella-like molybdenum dioxide consisting of nanosheets as an anode material for lithium-ion battery. *Electrochem. Commun.* **2008**, *10*, 118–122. [CrossRef]

186. Ponrouch, A.; Taberna, P.-L.; Simon, P.; Palacín, M.R. On the origin of the extra capacity at low potential in materials for Li batteries reacting through conversion reaction. *Electrochim. Acta* **2012**, *61*, 13–18. [CrossRef]
187. Gachot, G.; Grugeon, S.; Armand, M.; Pilard, S.; Guenot, P.; Tarascon, J.-M.; Laruelle, S. Deciphering the multi-step degradation mechanisms of carbonate-based electrolyte in Li batteries. *J. Power Sources* **2008**, *178*, 409–421. [CrossRef]
188. Grugeon, S.; Laruelle, S.; Herrera-Urbina, R.; Dupont, L.; Poizot, P.; Tarascon, J.-M. Particle Size Effects on the Electrochemical Performance of Copper Oxides toward Lithium. *J. Electrochem. Soc.* **2001**, *148*, A285–A292. [CrossRef]
189. Lee, S.W.; Yabuuchi, N.; Gallant, B.M.; Chen, S.; Kim, B.-S.; Hammond, P.T.; Shao-Horn, Y. High-power lithium batteries from functionalized carbon-nanotube electrodes. *Nat. Nanotechnol.* **2010**, *5*, 531. [CrossRef]
190. Jain, A.; Aravindan, V.; Jayaraman, S.; Kumar, P.S.; Balasubramanian, R.; Ramakrishna, S.; Madhavi, S.; Srinivasan, M. Activated carbons derived from coconut shells as high energy density cathode material for Li-ion capacitors. *Sci. Rep.* **2013**, *3*, srep03002. [CrossRef]
191. Kaneko, Y.; Park, J.; Yokotsuji, H.; Odawara, M.; Takase, H.; Ue, M.; Lee, M.-E. Cathode solid electrolyte interface's function originated from salt type additives in lithium-ion batteries. *Electrochim. Acta* **2016**, *222*, 271–279. [CrossRef]
192. Edström, K.; Gustafsson, T.; Thomas, J. The cathode–electrolyte interface in the Li-ion battery. *Electrochim. Acta* **2004**, *50*, 397–403. [CrossRef]
193. Yang, L.; Markmaitree, T.; Lucht, B.L. Inorganic additives for passivation of high voltage cathode materials. *J. Power Sources* **2011**, *196*, 2251–2254. [CrossRef]
194. Cherkashinin, G.; Nikolowski, K.; Ehrenberg, H.; Jacke, S.; Dimesso, L.; Jaegermann, W. The stability of the SEI layer, surface composition and the oxidation state of transition metals at the electrolyte–cathode interface impacted by the electrochemical cycling: X-ray photoelectron spectroscopy investigation. *Phys. Chem. Chem. Phys.* **2012**, *14*, 12321–12331. [CrossRef] [PubMed]
195. Lu, W.; Zhang, J.; Xu, J.; Wu, X.; Chen, L. In Situ Visualized Cathode Electrolyte Interphase on LiCoO2 in High Voltage Cycling. *ACS Appl. Mater. Interfaces* **2017**, *9*, 19313–19318. [CrossRef] [PubMed]
196. Tan, S.; Zhang, Z.; Li, Y.; Li, Y.; Zheng, J.; Zhou, Z.; Yang, Y. Tris (hexafluoro-iso-propyl) phosphate as an SEI-forming additive on improving the electrochemical performance of the Li[Li0.2Mn0.56Ni0.16Co0.08]O_2 cathode material. *J. Electrochem. Soc.* **2012**, *160*, A285. [CrossRef]
197. Omar, N.; Daowd, M.; Hegazy, O.; Al Sakka, M.; Coosemans, T.; Bossche, P.V.D.; van Mierlo, J. Assessment of lithium-ion capacitor for using in battery electric vehicle and hybrid electric vehicle applications. *Electrochim. Acta* **2012**, *86*, 305–315. [CrossRef]
198. Cao, W.J.; Zheng, J.P. The Effect of Cathode and Anode Potentials on the Cycling Performance of Li-Ion Capacitors. *J. Electrochem. Soc.* **2013**, *160*, A1572–A1576. [CrossRef]
199. Buqa, H.; Goers, D.; Holzapfel, M.; Spahr, M.E.; Novák, P. High-Rate Capability of Graphite Negative Electrodes for Lithium-Ion Batteries. *J. Electrochem. Soc.* **2005**, *152*, A474–A481. [CrossRef]
200. Sawai, K.; Ohzuku, T. Factors Affecting Rate Capability of Graphite Electrodes for Lithium-Ion Batteries. *J. Electrochem. Soc.* **2003**, *150*, A674–A678. [CrossRef]
201. Lisbona, D.; Snee, T. A review of hazards associated with primary lithium and lithium-ion batteries. *Process. Saf. Environ. Prot.* **2011**, *89*, 434–442. [CrossRef]
202. Wang, Q.; Ping, P.; Zhao, X.; Chu, G.; Sun, J.; Chen, C. Thermal runaway caused fire and explosion of lithium-ion battery. *J. Power Sources* **2012**, *208*, 210–224. [CrossRef]
203. Prada, E.; Di Domenico, D.; Creff, Y.; Bernard, J.C.; Sauvant-Moynot, V.; Huet, F. Simplified Electrochemical and Thermal Model of $LiFePO_4$-Graphite Li-Ion Batteries for Fast Charge Applications. *J. Electrochem. Soc.* **2012**, *159*, A1508–A1519. [CrossRef]
204. Maleki, H.; Howard, J.N. Role of the cathode and anode in heat generation of Li-ion cells as a function of state of charge. *J. Power Sources* **2004**, *137*, 117–127. [CrossRef]
205. Spitthoff, L.; Lamb, J.J.; Pollet, B.G.; Burheim, O.S. Lifetime Expectancy of Lithium-Ion Batteries. In *Micro-Optics and Energy*; Springer International Publishing: Cham, Switzerland, 2020; pp. 157–180.
206. Spitthoff, L.; Øyre, E.S.; Muri, H.I.; Wahl, M.; Gunnarshaug, A.F.; Pollet, B.G.; Lamb, J.J.; Burheim, O.S. Thermal Management of Lithium-Ion Batteries. In *Micro-Optics and Energy*; Springer International Publishing: Cham, Switzerland, 2020; pp. 183–194.
207. Lim, E.; Jo, C.; Kim, M.S.; Kim, M.-H.; Chun, J.; Kim, H.; Park, J.; Roh, K.C.; Kang, K.; Yoon, S.; et al. High-Performance Sodium-Ion Hybrid Supercapacitor Based on Nb_2O_5@Carbon Core-Shell Nanoparticles and Reduced Graphene Oxide Nanocomposites. *Adv. Funct. Mater.* **2016**, *26*, 3711–3719. [CrossRef]
208. Qu, Q.; Zhu, Y.; Gao, X.; Wu, Y. Core-Shell Structure of Polypyrrole Grown on V_2O_5 Nanoribbon as High-Performance Anode Material for Supercapacitors. *Adv. Energy Mater.* **2012**, *2*, 950–955. [CrossRef]
209. Li, L.; Peng, S.; Bin Wu, H.; Yu, L.; Madhavi, S.; Lou, X.W. (David) A Flexible Quasi-Solid-State Asymmetric Electrochemical Capacitor Based on Hierarchical Porous V_2O_5 Nanosheets on Carbon Nanofibers. *Adv. Energy Mater.* **2015**, *5*, 1500753. [CrossRef]
210. Chen, Z.; Augustyn, V.; Wen, J.; Zhang, Y.; Shen, M.; Dunn, B.; Lu, Y. High-Performance Supercapacitors Based on Intertwined CNT/V_2O_5 Nanowire Nanocomposites. *Adv. Mater.* **2011**, *23*, 791–795. [CrossRef]
211. Lukatskaya, M.R.; Mashtalir, O.; Ren, C.E.; Dall'Agnese, Y.; Rozier, P.; Taberna, P.L.; Naguib, M.; Simon, P.; Barsoum, M.W.; Gogotsi, Y. Cation intercalation and high volumetric capacitance of two-dimensional titanium carbide. *Science* **2013**, *341*, 1502–1505. [CrossRef] [PubMed]
212. Come, J.; Naguib, M.; Rozier, P.; Barsoum, M.W.; Gogotsi, Y.; Taberna, P.-L.; Morcrette, M.; Simon, P. A Non-Aqueous Asymmetric Cell with a Ti_2C-Based Two-Dimensional Negative Electrode. *J. Electrochem. Soc.* **2012**, *159*, A1368–A1373. [CrossRef]

213. Couly, C.; Alhabeb, M.; van Aken, K.L.; Kurra, N.; Gomes, L.; Navarro-Suárez, A.M.; Anasori, B.; Alshareef, H.N.; Gogotsi, Y. Asymmetric flexible MXene-reduced graphene oxide micro-supercapacitor. *Adv. Electron. Mater.* **2018**, *4*, 1700339. [CrossRef]
214. Wang, H.; Zhang, Y.; Ang, H.; Zhang, Y.; Tan, H.T.; Zhang, Y.; Guo, Y.; Franklin, J.B.; Wu, X.L.; Srinivasan, M.; et al. A High-Energy Lithium-Ion Capacitor by Integration of a 3D Interconnected Titanium Carbide Nanoparticle Chain Anode with a Pyridine-Derived Porous Nitrogen-Doped Carbon Cathode. *Adv. Funct. Mater.* **2016**, *26*, 3082–3093. [CrossRef]
215. Luo, J.; Zhang, W.; Yuan, H.; Jin, C.; Zhang, L.; Huang, H.; Liang, C.; Xia, Y.; Zhang, J.; Gan, Y.; et al. Pillared Structure Design of MXene with Ultralarge Interlayer Spacing for High-Performance Lithium-Ion Capacitors. *ACS Nano* **2017**, *11*, 2459–2469. [CrossRef] [PubMed]
216. Cabana, J.; Monconduit, L.; Larcher, D.; Palacín, M.R. Beyond intercalation-based Li-ion batteries: The state of the art and challenges of electrode materials reacting through conversion reactions. *Adv. Mater.* **2010**, *22*, 170. [CrossRef]
217. Ding, R.; Qi, L.; Wang, H. An investigation of spinel $NiCo_2O_4$ as anode for Na-ion capacitors. *Electrochimica Acta* **2013**, *114*, 726–735. [CrossRef]
218. Stephenson, T.; Li, Z.; Olsen, B.C.; Mitlin, D. Lithium ion battery applications of molybdenum disulfide (MoS_2) nanocomposites. *Energy Environ. Sci.* **2014**, *7*, 209–231. [CrossRef]
219. Wang, R.; Wang, S.; Jin, D.; Zhang, Y.; Cai, Y.; Ma, J.; Zhang, L. Engineering layer structure of MoS_2-graphene composites with robust and fast lithium storage for high-performance Li-ion capacitors. *Energy Storage Mater.* **2017**, *9*, 195–205. [CrossRef]
220. Aravindan, V.; Gnanaraj, J.; Lee, Y.-S.; Madhavi, S. Insertion-Type Electrodes for Nonaqueous Li-Ion Capacitors. *Chem. Rev.* **2014**, *114*, 11619–11635. [CrossRef]
221. Ping, L.; Zheng, J.; Shi, Z.; Qi, J.; Wang, C. Electrochemical performance of MCMB/(AC+ $LiFePO_4$) lithium-ion capacitors. *Chin. Sci. Bull.* **2013**, *58*, 689–695. [CrossRef]
222. Böckenfeld, N.; Balducci, A. On the use of lithium vanadium phosphate in high power devices. *J. Power Sources* **2013**, *235*, 265–273. [CrossRef]
223. Kong, L.; Zhang, C.; Wang, J.; Qiao, W.; Ling, L.; Long, D. Free-standing T-Nb_2O_5/graphene composite papers with ultrahigh gravimetric/volumetric capacitance for Li-ion intercalation pseudocapacitor. *ACS Nano* **2015**, *9*, 11200–11208. [CrossRef]
224. Lim, E.; Kim, H.; Jo, C.; Chun, J.; Ku, K.; Kim, S.; Lee, H.I.; Nam, I.-S.; Yoon, S.; Kang, K.; et al. Advanced Hybrid Supercapacitor Based on a Mesoporous Niobium Pentoxide/Carbon as High-Performance Anode. *ACS Nano* **2014**, *8*, 8968–8978. [CrossRef] [PubMed]
225. Divya, M.L.; Aravindan, V. Electrochemically Generated γ-LixV_2O_5 as Insertion Host for High-Energy Li-Ion Capacitors. *Chem. Asian J.* **2019**, *14*, 4665–4672. [CrossRef] [PubMed]
226. Lim, E.; Jo, C.; Kim, H.; Kim, M.-H.; Mun, Y.; Chun, J.; Ye, Y.; Hwang, J.; Ha, K.-S.; Roh, K.C.; et al. Facile Synthesis of Nb_2O_5@Carbon Core–Shell Nanocrystals with Controlled Crystalline Structure for High-Power Anodes in Hybrid Supercapacitors. *ACS Nano* **2015**, *9*, 7497–7505. [CrossRef] [PubMed]
227. Lai, C.-H.; Ashby, D.; Moz, M.; Gogotsi, Y.; Pilon, L.; Dunn, B. Designing Pseudocapacitance for Nb_2O_5/Carbide-Derived Carbon Electrodes and Hybrid Devices. *Langmuir* **2017**, *33*, 9407–9415. [CrossRef] [PubMed]
228. Wang, X.; Li, G.; Chen, Z.; Augustyn, V.; Ma, X.; Wang, G.; Dunn, B.; Lu, Y. High-Performance Supercapacitors Based on Nanocomposites of Nb_2O_5 Nanocrystals and Carbon Nanotubes. *Adv. Energy Mater.* **2011**, *1*, 1089–1093. [CrossRef]
229. Jiang, H.; Wang, S.; Zhang, B.; Shao, Y.; Wu, Y.; Zhao, H.; Lei, Y.; Hao, X. High performance lithium-ion capacitors based on $LiNbO_3$-arched 3D graphene aerogel anode and BCNNT cathode with enhanced kinetics match. *Chem. Eng. J.* **2020**, *396*, 125207. [CrossRef]
230. Wang, P.; Wang, R.; Lang, J.; Zhang, X.; Chen, Z.; Yan, X. Porous niobium nitride as a capacitive anode material for advanced Li-ion hybrid capacitors with superior cycling stability. *J. Mater. Chem. A* **2016**, *4*, 9760–9766. [CrossRef]
231. Wang, R.; Lang, J.; Zhang, P.; Lin, Z.; Yan, X. Fast and Large Lithium Storage in 3D Porous VN Nanowires-Graphene Composite as a Superior Anode Toward High-Performance Hybrid Supercapacitors. *Adv. Funct. Mater.* **2015**, *25*, 2270–2278. [CrossRef]
232. Liu, C.; Zhang, C.; Song, H.; Zhang, C.; Liu, Y.; Nan, X.; Cao, G. Mesocrystal MnO cubes as anode for Li-ion capacitors. *Nano Energy* **2016**, *22*, 290–300. [CrossRef]
233. Wang, H.; Xu, Z.; Li, Z.; Cui, K.; Ding, J.; Kohandehghan, A.; Tan, X.; Zahiri, B.; Olsen, B.C.; Holt, C.M.B.; et al. Hybrid Device Employing Three-Dimensional Arrays of MnO in Carbon Nanosheets Bridges Battery–Supercapacitor Divide. *Nano Lett.* **2014**, *14*, 1987–1994. [CrossRef]
234. Liu, C.; Zhang, C.; Song, H.; Nan, X.; Fu, H.; Cao, G. MnO nanoparticles with cationic vacancies and discrepant crystallinity dispersed into porous carbon for Li-ion capacitors. *J. Mater. Chem. A* **2016**, *4*, 3362–3370. [CrossRef]
235. Zhang, J.; Lin, J.; Zeng, Y.; Zhang, Y.; Guo, H. Morphological and Structural Evolution of MnO@ C Anode and Its Application in Lithium-Ion Capacitors. *ACS Appl. Energy Mater.* **2019**, *2*, 8345–8358. [CrossRef]
236. Liu, C.; Zhang, C.; Fu, H.; Nan, X.; Cao, G. Exploiting High-Performance Anode through Tuning the Character of Chemical Bonds for Li-Ion Batteries and Capacitors. *Adv. Energy Mater.* **2017**, *7*, 1601127. [CrossRef]
237. Li, M.; Pan, F.; Choo, E.S.G.; Lv, Y.; Chen, Y.; Xue, J.M. Designed Construction of a Graphene and Iron Oxide Freestanding Electrode with Enhanced Flexible Energy-Storage Performance. *ACS Appl. Mater. Interfaces* **2016**, *8*, 6972–6981. [CrossRef] [PubMed]
238. Brandt, A.; Balducci, A. A study about the use of carbon coated iron oxide-based electrodes in lithium-ion capacitors. *Electrochim. Acta* **2013**, *108*, 219–225. [CrossRef]

239. Zhang, F.; Zhang, T.; Yang, X.; Zhang, L.; Leng, K.; Huang, Y.; Chen, Y. A high-performance supercapacitor-battery hybrid energy storage device based on graphene-enhanced electrode materials with ultrahigh energy density. *Energy Environ. Sci.* **2013**, *6*, 1623–1632. [CrossRef]
240. Ding, R.; Qi, L.; Wang, H. Porous NiCo2O4 as an anode material for 4.5 V hybrid Li-ion capacitors. *RSC Adv.* **2013**, *3*, 12581. [CrossRef]
241. Karthikeyan, K.; Amaresh, S.; Aravindan, V.; Kim, H.; Kang, K.S.; Lee, Y.S. Unveiling organic–inorganic hybrids as a cathode material for high performance lithium-ion capacitors. *J. Mater. Chem. A* **2012**, *1*, 707–714. [CrossRef]
242. Cericola, D.; Novák, P.; Wokaun, A.; Kötz, R. Hybridization of electrochemical capacitors and rechargeable batteries: An experimental analysis of the different possible approaches utilizing activated carbon, $Li_4Ti_5O_{12}$ and $LiMn_2O_4$. *J. Power Sources* **2011**, *196*, 10305–10313. [CrossRef]
243. Arun, N.; Jain, A.; Aravindan, V.; Jayaraman, S.; Ling, W.C.; Srinivasan, M.P.; Madhavi, S. Nanostructured spinel $LiNi0.5Mn1.5O_4$ as new insertion anode for advanced Li-ion capacitors with high power capability. *Nano Energy* **2015**, *12*, 69–75. [CrossRef]
244. Karthikeyan, K.; Aravindan, V.; Lee, S.; Jang, I.; Lim, H.; Park, G.; Yoshio, M.; Lee, Y. Electrochemical performance of carbon-coated lithium manganese silicate for asymmetric hybrid supercapacitors. *J. Power Sources* **2010**, *195*, 3761–3764. [CrossRef]
245. Kaliyappan, K.; Amaresh, S.; Lee, Y.-S. $LiMnBO_3$ Nanobeads As an Innovative Anode Material for High Power Lithium-Ion Capacitor Applications. *ACS Appl. Mater. Interfaces* **2014**, *6*, 11357–11367. [CrossRef] [PubMed]
246. Li, F.-F.; He, Z.-H.; Gao, J.-F.; Kong, L.-B. The investigations of pyrophosphate $CoNiP_2O_7$ produced by hydrothermal process: A high-performance anode electrode material for Li-ion hybrid capacitor. *Ionics* **2020**, *26*, 2989–3001. [CrossRef]